INVESTIGATION OF THE SOLUTION CHEMISTRY AND DERMAL ABSORPTION OF NOVEL COPPER (II) CHELATING AGENTS THAT CAN SERVE AS POTENTIAL ANTI-INFLAMMATORY DRUGS.

By:

Kagiso Mokalane

MKLKAG 001

Thesis presented for the degree of Master of Science.

In the Department of Chemistry
University of Cape Town
Date: June 2011

Supervisor:
Prof. Graham E. Jackson

DECLARATION

I hereby declare that "I know the meaning of plagiarism and that all of the work in the document, save for that which is properly acknowledged, is my own".

ACKNOWLEDGEMENTS

I would like to express my sincere gratitude to the following:

My supervisor, Professor Graham E. Jackson, for his guidance and patience thought the course of this study.

My colleagues in the research group for their useful discussions.

Mr. Noel Hendricks, NMR operator, for assistance

National Research Foundation (NRF) for the financial assistance and support

CONFERENCE PROCEEDINGS

Parts of the thesis have been presented at the following conference: Inorg 2009, Bloemfontein

Topic-Potentiometric investigation of copper (II) based anti-inflammatory drugs

Abstract

The therapeutic/pharmacological effects of Copper (II) or its complexes with organic ligands have in the past three decades received much attention, and this is partly, because copper (II) complexes have been reported to be good in alleviating inflammation associated with rheumatoid arthritis. Therefore this study describes the investigation of the solution chemistry of the copper (II) complexes of homopiperazine and an adamentane derivative of homopiperazine (PCU.homo) using glass electrode potentiometry, UV/VIS spectroscopy, speciation modeling, nuclear magnetic resonance spectroscopy, blood plasma modeling, and dermal absorption.

Protonation, Cu(II) and Zn(II) complex stability constants were determined at 25˚C in 0.15 $mol.dm^{-1}$ $Cl^{-}(Na^{+})$ using a glass electrode. For PCU.homo-Cu(II), the MLH species predominated (reaching ≈ 80 %) under physiological conditions. The determination of the formation constants of PCU.homopiperazine-Zn(II) complex was complicated by the formation of a precipitate at high pH values (i.e. pH values ≥ 7).

The structures of the complexes formed in solution were determined using N M R. spectroscopy and UV/VIS spectroscopy. These results indicated that in the ML species only 3 amine donor groups are coordinated to the metal ion (i.e. MN_3-$[H_2O]_3$ type of coordination), while for the MLH species only one side of the ligand was coordinated to Cu(II). MM calculation supported the experimental structures.

The plasma mobilizing index of Cu(II)-(PCU.homo) complex was calculated using ECCLES (Evaluation of Constituent Concentration in Large Equilibrium System). The model showed that PCU.homopiperazine is not good in mobilizing copper *in vivo*, even at high ligand concentration.

Tissue permeability studies were performed using a modified Franz cell and a cerasome 9005 membrane, where, K_p (permeability coefficient) was found to be 5.06×10^{-6} cm/s (± 0.03). These results suggest that PCU.homopiperazine has the ability of improving dermal absorption of copper.

LIGAND ABBREVIATIONS USED

PCUA	-3.5-bis [ethanediamine]-4-[oxahexacyclododecane]
EN	-Ethylenediamine
Gly	-Glycinate
DTPA	-diethylenetriamine-N,N,N',N'',N''-pentaacetic aicd
EDTA	- Ethylenediaminetertraacetic acid
HP	- homopiperazine or 1,4diazacycloheptane
H(555-N)	-N-(2-(2-aminoethyl)ethyl)picolinamide
PCU.homo	-N, N'-bis [1, 4diazacycloheptane]-4-[oxahexacyclododecane]
PCU.EN	-N, N'-bis [ethylene diamine]-4-[oxahexacyclododecane]
Ttda	-3, 6, 9, 12-tetraazatetradecanedioic acid
Dtda	-N, N'-(bis [2-(dimethylamino) ethyl]-ethanediamine) H_2
PrDH	-N,N'-di(aminoethylene)-2,6-pyridine-dicarbonylamine
9aneN_3	-3, 6, 9-Triazaundecane

OTHER ABBREVIATIONS USED

R.A	–Rheumatoid arthritis
NSAIDs	-Nonsteroidal anti-inflammatory drugs
COX (II)	-Cyclo-oxygenase enzyme
DMARDs	-Disease- modifying anti-rheumatic drugs
SOD	-Superoxide dismutase
HSA	-Human serum albumin
CP	-Ceruloplasmin
UV	-Ultraviolet
VIS	-Visible spectroscopy
ESTA	-Equilibrium Simulation for Titration Analysis
T_H	-total proton concentration (mol/dm^3)
T_L	-total ligand concentration (mol/dm^3)
T_M	-total metal concentration (mol/dm^3)
K_W	-dissociation constant of water
E_{cell}	-electrode potential (volts)
E^o	-electrode response intercept (volts)
R	-universal gas constant ($JK^{-1}mol^{-1}$)
T	-absolute temperature (Kelvin)
F	-Faraday constant
$[H^+]$	-hydrogen ion activity
s	- Electrode slope
R_H	-Hamiltonian R-factor
$R_{lim}{}^H$	-Hamiltonian R-limit
OBJE	-Task to calculate object function

Z_H-bar	-Protonation function
Z_M-bar	-Complex formation function
Q-bar	-Deprotonation function
SPEC	-Task to calculate the speciation in solution
logβ	- log equilibrium constant (log beta)
p q r	- symbols representing the stochiometry of the reacting species
KHP	-Potassium hydrogen phthalate
2D NMR	- Two dimensional Nuclear Magnetic Resonance spectroscopy.
ECCLES	-Evaluation of Constituent Concentration in Large Equilibrium Systems
[L]	-free ligand concentration
p.m.i	-Plasma mobilizing index
l.m.w	-low molecular weight
λ_{max}	-frequency of maximum absorption
U_{total}	-total strain energy
$\sum E_b$	-total bond deformation energy
$\sum E_\Theta$	-total valence angle deformation energy
$\sum E_\Phi$	-total torsion (or dihedral) deformation energy
$\sum E_{nb}$	-total non-bonded (van der waals) interaction energy
r	-ideal bond length
Θ	-bond angle
Ø	-dihedral angle
r_{ij}	-inter-nuclear distance

Structural Formulae of ligands used or discussed in this Study

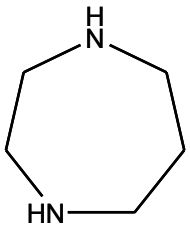

homopiperazine

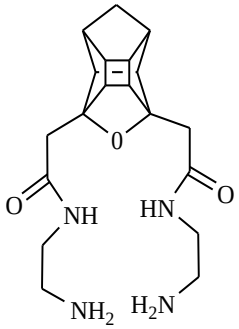

3,5-bis[ethanediamine]-4-[oxahexacyclododecane]
PCUA

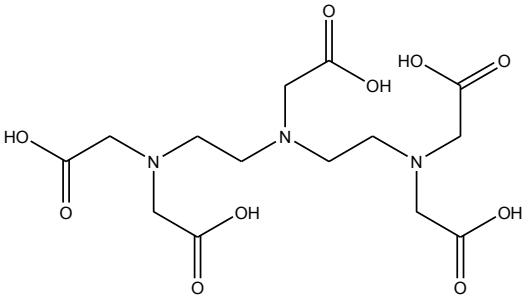

diethylenetriamine-N,N,N',N'',N-pentaacetic acid
DTPA

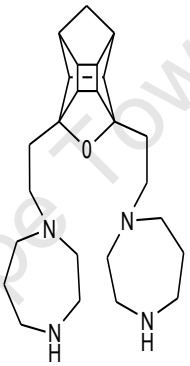

N, N'-bis[1, 4 diazacycloheptane]-4-[oxahexacyclododecane]
PCU.homo

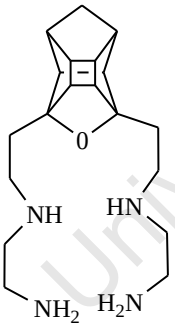

N, N'-bis[ethalene diamine]-4-[oxahexacyclododecane]
PCU.EN

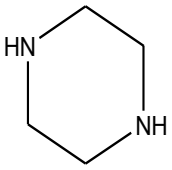

piperazine

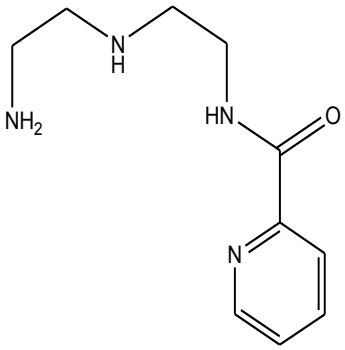

N-(2-(2-aminoethylamino)ethyl)picolinamide
[H(555-N)]

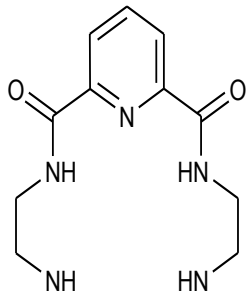

N, N'-di[amino ethylene]-2, 6- pyridine-dicarbonyline
PrDH

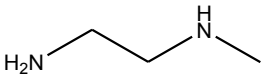

N^1-methylethane-1,2-diamine

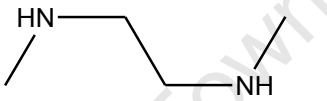

N^1,N^3-dimethylpropane-1,3-diamine

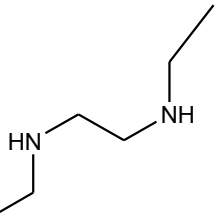

N^1,N^2-diethylethane-1,2-diamine

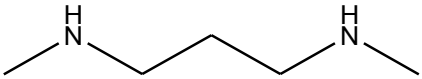

N^1,N^3-dimethylpropane-1,3-diamine

Contents

CHARPTER 1:

INTRODUCTION

1. RHEUMATOID ARTHRITIS

1.1 Introduction

Rheumatoid arthritis is a chronic, progressive disease in which inflammation changes occur throughout the connective tissues of the body [1], with its symptoms appearing in the same joints on both sides of the body. Joints that are susceptible to RA attack include joints of fingers, wrist (as shown in Figure 1.1), elbows, knuckles and knees [1].

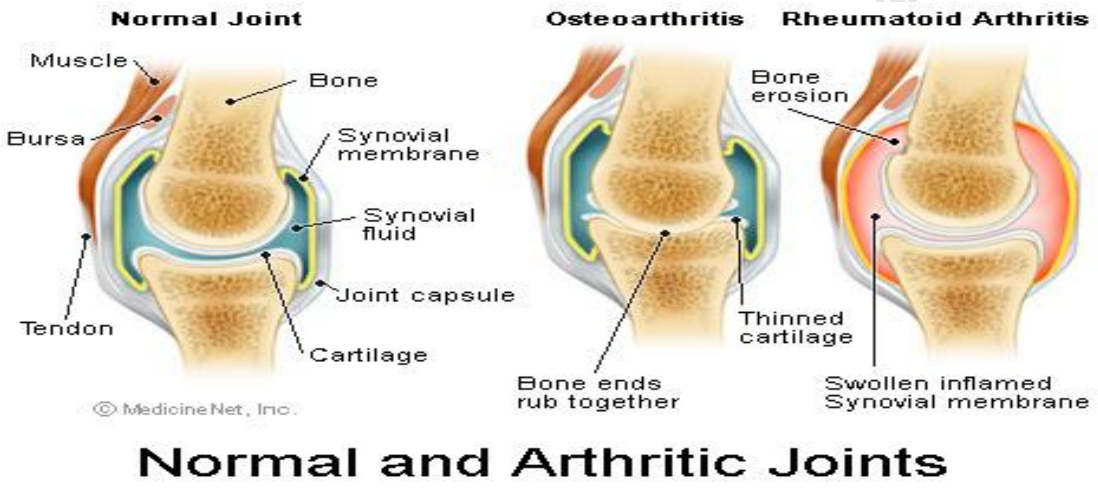

Figure 1.1 picture of a hand affected with RA

Rheumatoid arthritis has been reported to affect 5% of the population of developing countries, with 50% of these cases reported as acute infections [2]. It normally attacks people between the ages of 25 and 50 and it has been reported as being more prevalent in women than in men [1-2]. It has also been found to occur in children where it is referred to as juvenile poly-arthritis [1, 3]. The disease is believed to be caused by a faulty autoimmune response where hydrolytic enzymes which include, collagenases, proteases, gelatinases and matrilysin are released inside cells present at the sites of tissue injury, and this results in the degradation of collagen and other structural components that form part of the joint, this then leads to severe tissue destruction, and joint

damage (see Figure 1.1) [4]. This follows from the fact that 90% of the reported cases of people diagnosed with rheumatoid arthritis have been found to contain high levels of a certain autoantibody in their blood serum [4]. This autoantibody (auto-immunoglobin) is called Rheumatoid factor. The specific antigen that causes this cascade (autoimmune response) of reactions is still not known [1, 3, 5-6].

Even though RA is generally referred to as a joint disease (synovitis) its symptoms may manifest in ways not directly associated with the joints [1-2]. This includes: blood-vessel inflammation in the form of necrosis in the fingertips, chronic leg ulcers and lesions in the peripheral nerves, inflammation and nodule formation in the lungs and pleura (tissue covering the lung) [1].

1.2 Treatment of symptoms of Rheumatoid Arthritis

There is no cure for this debilitating disease [5]. This is mainly due its poorly understood pathogenic mechanism [2-3]. However the disease is controlled by immunosuppressive drugs and its symptoms are treated with anti-inflammatory drugs [1-3]. An effective treatment program for arthritis involves drug therapy (steroidal or non-steroidal drugs), exercise and rest [5]. In most cases of RA, patients have complete remission and exacerbations of the symptoms [6], therefore early therapy is very important in relieving the early symptoms associated with RA [4]. Appearance of subcutaneous rheumatoid nodules in the shoulder joint can also help to diagnose the disease faster [1, 6]. Surgery is often of value in correcting established joint deformities [4, 6-7]. Therapeutic/ anti-inflammatory drugs that are normally given to treat R.A. patients fall into three categories; discussed in the next sections.

1.2.1 Nonsteroidal anti-inflammatory drugs (NSAIDs)

Nonsteroidal anti-inflammatory drugs (NSAIDs) are reported to form the first line of anti-rheumatic drugs [6-7]. NSAIDs have analgesic, antipyretic and anti-inflammatory properties.

They are thought to reduce inflammation and pain by inhibiting the activity of cyclo-oxygenase enzyme [7]. Cyclo-oxygenase has been linked to the catalytic production of pro-inflammatory immunoglobulins called prostaglandin (PG's) and leukotriennes in the synovial cells by oxidizing arachidonic acid [7]. Examples of NSAIDs include Ibrufen, Naproxen and Diclofenac sodium (Voltaren). Ibrufen and Voltaren have been recommended by clinics for pain relief, and to reduce inflammation in RA if taken in full doses [5]. The recommended dosage is 1200 to 3200 milligrams per day in 3 or 4 doses and 100 to 200 milligrams per day in 2 and 3 doses respectively [5]. However the continued use of these types of drugs results in severe side effects, such as gastrointestinal ulcers, and kidney damage. NSAIDs have also been reported to interfere with the repair of superficial injury and suppression of gastric prostaglandin synthesis [5-8]. To try and improve the effects that NSAIDs have on the stomach lining, new drugs have been developed as alternative for NSAIDs [7-8]. They are called cyclooxygenase-2 (COX-2) inhibitors which are milder on the stomach lining [7-8]. However the setback of these drugs is their inability to change the outcome of the disease [8].

1.2.2 Glucoticosteroids

The use of adrenal corticosteroid (sometime referred to as simply steroids) has been reported to produce dramatic improvement on the disease, but its effectiveness is reported to diminish with time [4-6]. The use of this hormone like molecule is reported to have both metabolic and physiological effects such as increased susceptibility to further infections, appearance of peptic ulcers, affecting lymphocytes, granulocytes and as well as inhibiting the immune system [4, 6, 9]. It first received popularity as a symptomatic drug in the 1950s after Hench *et al.* reported its dramatic effect in reducing the symptoms of RA [8, 10].

Cortisone has been reported to bring relief to the symptoms of RA, but has received criticism from long term suffers of RA because of its undesirable long term effect [6, 8-9]. However its

use as part of a proper anti-rheumatic therapy has been reported as valuable during the treatment of arthritis. The required dosage is 5 mg to 7.5 mg per daily dose of cortisone, which is administered via injection. It is normally given to women after child birth [5, 7].

1.2.3 Disease modifying anti-rheumatoid drugs (DMARD)

There is a second line of anti-rheumatic drugs that has been reported to produce durable remissions and delay or halt diseases progression by diverting the course of the pathologic reaction associated with rheumatoid arthritis (RA) [6-8]. These include use of low dosages of azathioprine, cyclosporin (cyclosporine A), D-penicillamine, gold salts, hydroxychloroquine, Leflunomide, Methotrexate, Minocycline, and biological agents [6, 8].

These drugs can be divided further into two classes namely: disease modifying antirheumatic drugs (DMARDs) and biologic agents [7-8]. DMARDs are often required to reverse the disease process and prevent long-term damage [8]. In particular they prevent bone and joint damage from occurring secondary to the uncontrolled inflammation [8]. Classic examples of DMARDs include methotrexate and sulfasalzine [7-10]. Early therapy with methotrexane has been reported as being effective in stopping the early process of RA, which involves the joints being infiltrated by cells of the immune system that signal to one another and are thought to set up a self-pertuating chronic inflammation [3-4]. Biological agents are a new type of drug that decrease or stop the progress of RA [10]. They act as response modifiers that block specific immune factors that lead to RA [10]. This is following the recognition of prostaglandins (PG's) as an important component of the body's inflammation reaction. People who do not respond well to the first with DMARDs treatment are given an option to use protein-A immuno adsorption (Prosorba) therapy. Other examples of these biological agents include tumour necrosis factor alpha (TNFα) blockers, Infliximab (Remicade), and adalimab (Humira) [5, 10]. The problem with these new drugs is that they are still too expensive [1, 6, 10].

1.3 Background to study

1.3.1 Metals in living systems

Trace metal ions are important in the normal functioning of both plants and animals [12]. Examples include cobalt, copper, iron, nickel, molybdenum, selenium and zinc [9]. Some of their roles include taking part in metabolism and growth processes or forming part of the skeletal system of biological molecules, such as Co(I) in vitamin B12, and Fe(II) in haemoglobin. They can also be used to disrupt skeletal structure of biological molecules such when they are used in anti-bacterial agents [9]. However metal ion requirement by plant and animals species varies greatly from species to species [9, 12]. Much of the energy expended by an organism is used to maintain the correct concentration and speciation of metal ions in different cells. This is called homeostasis [9, 12-13]. A change in metal ion speciation may result in poor health or even retarded growth in some organisms [12]. Imbalances in metal homeostasis can also be caused by external factors such as smoking and the over use of prescription medication [11-12]. As a result a number of disorders occurring in humans have been linked or associated to levels of trace metals found in the body, with the disease controlled by either replenishing the specific metal ion concentration in the body from an exogenous source or by removing the excess metal ion from the body using a specific metal chelating agent [13]. Examples include lung and breast cancer which have been associated with low levels of selenium, Wilson disease which results in an accumulation of copper in the tissues of the liver, brain and kidneys [4, 9]. The symptoms of Wilson's disease can be treated with a daily dose of 50 milligrams of zinc taken with each meal; zinc is reported to effectively lower the abnormal accumulation of copper in people afflicted with this genetic disease of copper metabolism. Other examples include kidney stone formation which is associated with an imbalance between calcium and magnesium levels [17].

There are metals that are not essential and are toxic, but still manage to find their way into the body of living systems [16-17]. This is mainly caused by human's bad environmental management practices. Examples of these nonessential elements include lead, cadmium, and mercury. Out of all the trace elements described in the literature, copper is the metal which is mostly associated with the development of many metal dependent disorders occurring in the human body, examples include RA and enkephalins [14-17].

1.3.2 Bio-distribution of copper (II) and the involvement of copper (II) in RA.

Copper was first recognised as an essential element in 1921, after copper salts were shown to be active against anemia which was caused by a copper defiencient diet in animal models [9-10]. Since then scientists in this field of chemo-therapy agree on two facts when designing or developing novel therapeutic/chemotherapeutic agents. These include: knowledge of what happens at the molecular level during the onset of the disease is of value (i.e. Knowledge of how the body functions at the molecular is very important) [9-10] and that for a metal ion to be able to perform its biological role it must be bioavalable (i.e. it must be in a state/form were the body can access it). Essential metals such as zinc, copper, and iron achieve these by binding to some sort of a biological molecule normally apoproteins or apoenzymes. Copper in nature exists in three oxidation states, Cu(I), Cu(II) and Cu(III) [9, 10]. Like other essential amino acids, fatty acids, or vitamins, copper is not synthesized in the body and sources of this essential nutrient include dried beans, nuts, animal liver, and crustacean [4, 9]

The body contains between 50 and 120 milligrams of copper [10, 11]. Copper from an exogenous source, enters the body via rapid absorption through the stomach and small intestine (jejunum) by a facilitated diffusion, using transport proteins to help copper to pass-through the phospholipid membranes and it is finally stored in the liver via ligand exchange processes in the form of metallothionine complex [11-13]. Almost all of the copper found in the body is reported

to be bound either to transport proteins (ceruloplasmin and serum albumin), storage proteins (metallothioniens) or copper containing enzymes and low molecular weight complexes of copper [9]. It also forms part of our most important antioxidant enzymes, copper- zinc superoxide dismutase [9]. Other important functions of copper in the body include bone formation, keratinisation, reproduction, fertility, development of central and peripheral nervous systems, cardiac function, cellular respiration, nerve function, extracellular connective tissue formation, pigmentation and regulation of monoamine concentration [4, 8-9]. The amount of copper in each tissue correlates with the number and kind of metabolic processes requiring copper in that particular tissue [3, 6-7]. Excess copper is moved out of the body though biliary excretion [3, 7-8]. Furthermore these biological roles of copper are dependent on copper existing as a complex at the active site following complexation to a specific enzyme or protein [5-7]. Even though the stored copper-complexes are normally released by the liver into the blood to fulfil metabolic needs, they are also reported to be released as part of an acute-phase response during many disease states [6, 8, 9, 10, 14].

The medicinal property of copper and the anti-inflammatory agent salicin has been known for more than a century [5]. However interest in the beneficial effects of copper (II) complexes was renewed by Sorenson's report in 1976, which stated that the active forms of anti-inflammatory drugs are their Cu-complexes of such drugs *in vivo.* These analogues were also reported to be more active than their parent drug or inorganic copper salts [16]. The use of copper bangle to suppress inflammation associated with RA has been known for a very long-time [4, 9, 10]. Walker *et al*. have measured the dermal absorption from these bracelets and found it to be significant [6]. .

In metal-tissue distribution studies of copper in individuals with rheumatoid arthritis, elevated levels of serum copper were found during the inflammatory stage of the disease [14-16]. A two to three fold increases in endogenous copper, mainly serum albumin and ceruloplasmin (CP)),

was found in the blood of these individuals and this has been linked to the severity of the disease state [11, 17]. Furthermore the accumulation of copper-thionine in the liver decreases [11, 17, 18]. Since serum copper-containing components are synthesized in the liver and appear in serum after the onset of the disease, it seems reasonable to suggest that this is a physiologic response to arthritis, which facilitates remission [11, 12].

The l.m.w copper complexes are believed to be involved in the transportation of copper between cells in the body; this is because they are formally uncharged [11]. Furthermore, it is the decrease of these copper complexes in the body that is thought to increase the progression of RA. L.m.w copper complexes are also reported to have superoxide dismutase activity by controlling the hydroxide and superoxide radical levels in the blood serum [12]. Hydroxide and superoxide radicals have been associated with development inflammation in tissues [6, 9, 11, 12]. Some of the other functions performed by low molecular weight complexes include acting as intermediates in the process of metal ions release from the storage metalloenzymes, controlling redox potential and keeping metal ion in solution [11].

Ceruloplasmin has been reported to bind copper irreverserblily and therefore can be used in the transport of copper, but this will require denaturing of the protein at the injury site/target cell in order to release the metal [13]. This copper transport process has been reported to be dependent on copper redox activity (i.e. Cu(II) to Cu(I))[12, 13]. However the denaturing of the protein has severe side effects as ceruloplasmin has been shown to be involved in preventing cellular destruction; this is thought to account for the sudden increase of this protein in the blood during RA [12, 14]. Because of the increased interest in the role of l.m.w-copper complexes as potential anti-inflammatory agents a series of review papers have been published [14, 15], describing the synthesis of low molecular weight compounds that posses the potential of behaving as anti-inflammatory drugs. Examples of this compounds include indoles, hydroxyquinoline (Cu(II)-8-dimethyl ammonium sulphonate$_2$) also known as dicuprane, (cupramine, [Cu(I) (3-

allylthiouredobenzoate], and copper salicylates [2]. It was suggested that copper complexes of clinically used anti-arthritic drugs are responsible for the beneficial anti-arthritic effects of these drugs [16]. This is supported by the early observation by Sorenson's that copper complexes of many non-anti-inflammatory complexing agents have anti-inflammatory activity in animal models. This includes amino acids, amines and heterocyclic carboxylic acids. In addition some copper complexes of anti-arthritic drugs were also reported to show superoxide dismutase (SOD)-like activity *in vivo*, with decreased progression of RA and relatively low gastrointestinal toxicity in animal models compared to the normally used parent drugs [5, 11-19]. Examples of these anti-arthritic drugs include penicillamine and 1-phenyl-5-aminotetrazol [16]. It is worth mentioning that the anti-inflammatory activities reported for the compounds mentioned above were obtained via direct injection of the copper complexes into the blood of the studied rats [16].

Even though these drugs have been known for a long period of time, little is known about how they regulate inflammation and copper metabolism. Care has to be taken when using copper (II) complexes as they have been implicated as catalysts in the formation of deleterious $OH^{\cdot}$ radicals in the Fenton reaction in the foot oedema model [12].

There are several possible biochemical mechanisms that can account for the anti-inflammatory activity of copper (II) complexes. These include:

Inducing lysyl oxidase activity (enzyme involved in the tissue repair process), this follows the observation that low levels of lysyl oxidase enzyme are present in a copper deficient chicken and its activity was increased by injecting the chicken with exogenous copper (II) sulphate salt.

The modulation of protastagladin synthesis by decreasing the production of a pro-inflammatory prostaglandin PGE_2. Inducing or mimicking superoxide dismutase activity (see discussion

above). Decreasing the permeability of human synovial lysosome and modulating the physiological effect of histamine [2].

In order to improve the bioavailability of copper and hence improve the efficacy of these complexes, Jackson *et al* have investigated the systems of [Zn(II), Ca(II), Gd(III), and Cu(II)-(1,15-bis(N,N-dimethyl)-5,11-dioxo-8-(N-benzyl)-1,4,8,12,15-pentaazapentadecane)] (L^a). L^a was found to form more stable complexes with Cu(II) [18]. This high stability of the complex was attributed to the ease with which copper deprotonates the donor nitrogen atom of the amide groups. Although the Cu(II)-L^a complex was neutral under physiological conditions, it was reported to be hydrophilic and plasma model (*in vivo)* calculations revealed that the complex will dissociate in blood plasma [18]. This meant that further work was needed to improve the lipophilicity of this ligand and the stability of the resulting copper-complexes. Therefore ligands Ttda and Dtda were synthesised and their solution chemistry investigated against copper (II). It was reported that Ttda (β_{110} = 21.36) formed more stable complexes with copper (II) than Dtda (β_{110} = 19.16), but it was found that Ttda was too hydrophilic. Therefore resulting in the complex being readily excreted in urine while still intact [19]. However all was not lost as this drug could be used in the treatment of Wilson's disease due to the high affinity of this ligand for copper (II) *in vivo*. Dtda on the other-hand was reported to form weaker complexes than expected. This was accounted for by the ring strain that occurs in the macro-cycle, which is caused by the distorted geometry around the copper (II) ion [19]. As a result the complex was reported to dissociate *in vivo* and was excreted slowly via the liver. It was also suggested that the presence of an amide group provided a site for the addition of more hydrophobic groups that could help increase the ligand's liphophilicity [19]. In view of the circumstantial evidence surrounding the use of copper in the treatment of the inflammation accompanying RA, we have embarked on a search for similar chemical agents (i.e. polyamine ligands, see Figure 1.2) that will bind copper

selectively and be able to transfer the metal ion complex across cell membranes to the sites where it will exert its pharmacological activity.

1.4 Ligand properties and design

According to our hypothesis, for an agent to be accepted as an anti-inflammation drug, it must be able to increase the supply of copper to the sites of injury (i.e. increase concentration of free labile copper in the synovial fluid). It must, therefore, fulfil certain design requirements discussed below:

Looking at the complexity of the human body, firstly the copper chelating agents must be able to bind copper (II) selectively, without disrupting the homeostasis of the other trace metals found in the body and it must also form lipophilic complexes with copper so that it can cross bio-membranes.

The ligand must be able to form labile complexes with copper so that the copper can be released when required.

The ligand must also be a strong chelator of copper, but one needs to be careful that the ligand is not too strong a binder of copper, because it might end up being excreted with copper still bound to it.

To increase its selectivity for the binding of copper (II), the ligand must have predominantly nitrogen donor atoms (see Figure 1.2). This is because Cu(II) is a soft/borderline HSAB acid while its major *in vivo* competitors, Ca(II) and Zn(II) are hard acids. Thus the use of nitrogen donor ligands, as opposed to oxygen donor ligands will be favour the complexation of Cu(II). Sulphur donor ligands are avoided because they tend to be toxic.

If the agent is to be administered dermally it must be able to be absorbed through the skin. For this to happen, the complex must not be too lipophilic or too hydrophobic. If it is too hydrophobic it will not be able to pass through the stratum cornea. On the other hand, if the copper (II) complex is too lipophilic, it will become trapped in the underlying tissue.

The ligand system in this study is based on a penta-cycloundecane amine derivative (Figure 1.2), which is a triene moiety linked to a rigid cage via an ethylene bridge. The ligand system of the ON_4 type is capable of donating four nitrogen atoms (i.e. secondary amine groups) to a metal ion centre. The rigid cage structure on the ligand is expected to increase the lipophilicity and may also increase the stability of the metal complex by forcing the divalent metal into its favourable coordination geometry (see Figure 1.5) [2]. This is expected to drive the equilibrium towards complex formation [20, 21].

1.5. Ligand systems used in this study:

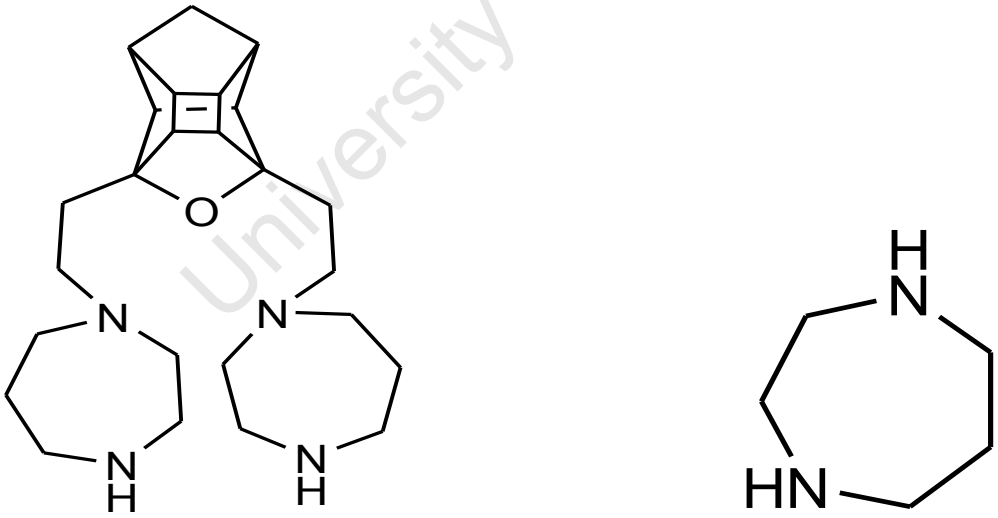

Figure 1.2: Structure of PCU.homopiperazine (pentacycloudecane,-bis1, 2-1,4diazacycloheptane) and homopiperazine (1, 4diazacycloheptane)

1.6 AIMS:

To develop novel copper based anti-inflammatory drugs that can be absorbed dermally.

Objectives:

1. Design a ligand which forms stable, labile copper complexes with high a level of specificity for copper binding and which is still able to diffuse across a lipid bilayer membrane (see Figure 1.2).
2. Synthesis the designed ligand.
3. Determine the protonation and complexation constants of PCU homopiperazine against Cu (II) and Zn (II) using a reversible glass electrode in an aqueous solution of 0.15 M (Na^+ Cl^-) over a pH range: 2-11.
4. Determine the structure of the metal complexes using NMR and UV/VIS spectroscopy studies.
5. Verify these structures using computational studies (MM calculations).
6. Calculate the *in vivo* speciation of copper using p.m.i/blood plasma model studies.
7. Determine the dermal absorption of the copper (II) complex at physiological pH using a modified Franz cell, and to calculate their partition coefficients.
8. Compare the results with homopipirazine, the cage free ligand (Figure 1.2)

Reference:

1. M. D. J. Freeman, Arthritis: The new Treatments. Contemporary books Inc(1979). Chicago.
2. O .Sebusi and G. E. Jackson, department of chemistry uct, masters dissertation (2003) on thermodynamic properties of diamino-diamide ligand as a –potential anti-inflammatory agent.
3. O. Sebusi., G. E. Jackson., T. Govender, H. G. Krugerb and A. Singh: Chemical speciation of copper (II) diaminediamide derivative of pentacycloundecane- a potential anti-inflammatory agent. Dalton Trans., 2007, p. 1140-1149.
4. J. E. Weder , C. T. Dillon , T. W. Hambley , B. J. Kennedy, P. A. Lay , J. R. Biffin , H. L. Regtop , N. M. Davies -Copper complexes of non-steroidal drugs.- a Centre for Heavy Metals Research, School of Chemistry, University of Sydney, Sydney NSW 2006, Australia.
5. I. Sanz, D. Alboukrek., In: Rheamatoid Arthritis. M. Fischbach(ed.) (1991), Churchill Livingstone, New York Edinburg.
6. http://www.connecticutcenterforhealth.com/rheumatoid-atrthritis
7. N. J. Zvimba, and G. E. Jackson, Copper chelating anti-inflammatory agents N^1-(2-aminoe ethyl)-N^2-(pyridin-2-ylmethyl)ethane-1, 2-diamine ([555-N]) and *N*-(2-(2-aminoethylamino) ethyl) picolinamide ([H (555)-N]) a *in vitro* and *in vivo* study. J. inorg. Biochem, 101 (2007) p. 148-158.
8. L. S. Simons and J.A. Mills: new Engl. J. Med. 302 (1980) p.1179-1185.
9. J. C. Frolich., Trends Pharmacol. Sci., 18 (1997) p. 30.
10. I. L Bonta., M. J. Parnham., J.E Vincent., P.C., Bragt, In: G.P. Ellis, G.P. West. Progress in Medicinal Chemistry, North Holland Biomedical Press (Eds.) (1980), North Holland, p. 185.

11. J. G Hardin., G.L Longenenecker, Handbook of Drug Therapy in Rheumatic Diseases, 1st ed, 1992.Little,Brown and Company, London.
12. C. Furnival., P. M. May and D.R. Williams. Trace Elements in the Pathogenesis and Treatment of Inflammation. K.D.Rainsford, K.Brune and M.W.Whitehouse (Eds), Birkkhauser Verlag (1981), Basel Boston Stuttgart.
13. J.R.J.Sorenson in metal ion in biological systems, volume 14. H. Sigel(Ed) (1982), Marcel Decker, New York.
14. N. J. Zvimba, and G. E. Jackson, Copper chelating anti-inflammatory agents N^1-(2-aminoe ethyl)-N^2-(pyridin-2-ylmethyl) ethane-1, 2-diamine ([555-N]) and *N*-(2-(2-aminoethylamino) ethyl) picolinamide ([H (555)-N]) a *vitro* and *in vivo* study. J.inorg Biochem 101 (2007) p. 148-158.
15. P. May and P. J. Linder. Chem.Soc.Daton Trans.1977, 1, p. 588-595.
16. J. R. J. Sorenson. The Anti-Inflammatory Activities of Copper Complexes
17. B.L. O'Dell, in Trace elements in Human Health and disease, Vol. 1 Zinc and copper (A.S Prasad and D. Oberleas, ends.), Academic Press1976, p 391, New York.
18. E.T. Nomkoko, G.E. Jackson, S.B. Nakani and R. Hunter. Solution chemistry of 1,15-bis(N,N-Dimethyl)-5,11-dioxo-8-(N-benzyl)-1,4,8,12,15-pentaazapentadecane with metal ions of biological interest-Insights toward active metal ion containing therapeutics and diagnostic agents. Dalton Trans (2006), p. 4029-4038.
19. M. Kelly, and G. E. Jackson, Department of Chemistry UCT, Thesis submitted for PHD (1998). Metal ion Equilibria in biofluids-Copper and Rheumatoid Arthritis
20. D. E. Golgberg and C. W. J Fernelius. Phys. Chem. 63 (1959), p. 1246-1249.
21. R.D.Hancock, J.Chem. Soc Dalton, (1980), p.416

CHARPTER 2

POTENTIOMETRY

2.1 Introduction

In the study of metal ion coordination equilibria in biological systems, the use of stability constants can readily provide a means of approximating the speciation of the metal ion of interest within the system [1]. The most widely used technique for the measurement of metal—complex stability constants is based on pH—metric titrations of a ligand in the absence and or in the presence of metal ions.

Several experimental methods, including some spectroscopic techniques, can be utilized to investigate the chemical speciation occurring in solution. Examples include ultra filtration, calorimetry, solvent extraction, potentiometry, reaction kinetics, nuclear magnetic resonance, Raman, UV/VIS and infrared spectroscopy [2]. From all these techniques mentioned above potentiometry is probably the oldest and most extensively used because of the easy availability of the electrodes, high sensitivity and reproducibility of experimental results, making it the most precise and accurate non-invasive technique available at present [2, 3].

2.2 Complex formation

The theory of complex formation and the potentiometric determination of stability constants have been dealt with extensively in literature [4]. Thus only a brief description of the reactions, equations and assumption that are applicable will be given here. Interest in formation of metal complexes in aqueous solution has evolved from interpreting the mechanism of formation and correlating stability constant data, to numerous applied fields ranging from sewage treatment to designing of metal ion buffers for use in biological systems [5-6].

Consider a general metal-ligand complex formation at equilibrium involving M, as a metal and L as a ligand.

The stepwise formation of different complexes can be described by the following set of formation constants. The charges are omitted for clarity.

$$M + L \rightleftharpoons ML \qquad K_1 = [ML]/[M][L] \qquad (2.2.1)$$

$$ML + L \rightleftharpoons ML_2 \qquad K_2 = [ML_2]/[ML][L] \qquad (2.2.2)$$

$ML_{n-1} + HL \rightleftharpoons ML_n + H$ $\quad K_n = [ML_n][H]/[ML_{n-1}][HL]$ (2.2.3)

The equilibria represented by equations 2.2.1, 2.2.2 and 2.2.3 can also be expressed as overall formation constants, denoted by β, and these are given below [4-5].

$M + L \rightleftharpoons ML$ $\quad \beta_1 = K_1 = [ML]/[M][L]$ (2.2.4)

$M + 2L \rightleftharpoons ML_2$ $\quad \beta_2 = K_1.K_2 = [ML_2]/[M][L]^2$ (2.2.5)

Thus, the stability constants in 2.2.4, 2.2.5 and 2.2.6 are related to the overall stability constant by the general expression

$$\beta_n = \prod_{i=1}^{n} K_i \qquad (2.2.6)$$

In any solution containing metal ions M, ligand and protons/hydroxyl ions H, a variety of complexes can be formed. This phenomenon occurring in solution can be described by the following general equilibrium equation [4, 5, 6].

$pM + qL + rH \rightleftharpoons M_pL_qH_r$ (2.2.7)

Where p, q and r are the stoichiometric coefficients for metal, ligand and proton respectively, while r = -1 refers to the proton being removed or the addition of a hydroxyl ion on the complex. Therefore this equation can take into account formation of mononuclear, binary, protonation or hydroxo, polynuclear as well as oligonuclear complexes [3]. However accurate determination of formation constants for this complex formed in aqueous solution is reported to be in terms of thermodynamic formation constant [2-6], and is defined as follows;

$${}^{T}\beta_{pqr} = \{M_pL_qH_r\}/\{M\}^p\{L\}^q\{H\}^r \qquad (2.2.8)$$

Were ${}^{T}\beta_{pqr}$ is the thermodynamic formation constant; and {} denotes the activities of the different chemical species participating in complex formation [4]. However, since activity of any chemical species in solution is given by the product of its concentration and activity coefficient (γ), for example $\{ML\} = \gamma_{ML}[ML]$ [4]. Therefore this equation for ${}^{T}\beta_{pqr}$ can be rewritten in terms of concentration and activity coefficients of the reacting species as follows;

$^{T}\beta_{pqr} = [M_pL_qH_r]/ [M]^p [L]^q [H]^r * \gamma_i$ (2.2.9)

Were [M], [L] and [H] are the concentrations for metal, free ligand, proton respectively and γ_i quotient of activity coefficients respectively. To avoid the complications involved in using or monitoring activities of different species in solution, thermodynamic formation constants are determined where possible in a solution of a background electrolyte at high ionic strength. Under these conditions, activity coefficient (γ) of an ion can be assumed to be constant [4-5]. Therefore $^{T}\beta_{pqr}$ can be expresed interms of concetration as follows:

$^{c}\beta_{pqr} = [M_pL_qH_r]/ [M]^p [L]^q [H]^r$ (2.2.10)

Thus by applying the mass action equation, the concentration of any complex formed in solution at equilibrium is governed by the relative total concentration of each component taking part in its formation, and the relative strength of the individual complexes (i.e. β_{pqr}) in solution [3, 4, 6], therefore:

$[H]^{-r} = \beta_{pqr} [M]^p [L]^q /[M^pL^qH^r]$ (2.2.11)

Similarly the total ligand and proton concentration solution, T_L and T_H will be given by the following equation according to the law of mass balance;

$T_L = [L] + q \sum\beta_{pqr}[M]^p [L]^q [H]^r$ (2.2.12)

$T_H = [H] + r \sum\beta_{pqr}[M]^p [L]^q [H]^r$ (2.2.13)

Where $[M]_p$ is the concentration of free aquated metal ions and the summation is over the concentration of all the metal containing species which may be protonated (r>0) or may not (r=0), while [L] and [H] represent the concentration of the uncomplexed ligand, proton respectively. In order to calculate the stability constants (β_{pqr}) from potentiometric data, the mass balance equations must be solved. In these equations, the total component concentrations (i.e. T_L, T_M and T_H) are known from the experimental procedure. The unknowns include the β's, free hydrogen ion concentration, free metal and free ligand concentrations, but the latter two physicochemical parameters can be determined by solving the mass action equations. If there are n_p titration

points and $n_{.m.b.e}$ mass balance equations at each point, then there will be a total of (n_p x $n_{.m.b.e}$) free concentrations.

The position of equilibrium and hence the numerical value of the reported stability constant when expressed in concentration units is normally dependent upon the temperature and this is given by the van't Hoff equation [3-7]:

$$\text{Log } K = \Delta H^\circ/RT^2 \qquad (2.2.14)$$

Were: R =universal gas constant, T = absolute temperature and ΔH° is the standard enthalpy. Thus for exothermic reactions (i.e. $-\Delta H^\circ$) K decreases with temperature, conversely endothermic (i.e. $+\Delta H^\circ$) K increases with temperature [4, 5].

.

2.3 Glass Electrode Potentiometry (GEP)

Virtually all equilibrium process taking place in aqueous solution involve hydrogen and hydroxyl ions whether directly or indirectly and therefore it is this ion's activity which is measured in glass electrode potentiometric investigations [4]. Furthermore this has resulted in glass electrode potentiometry (GEP) having found its significant place in the investigation of many chemical systems in biological, medical and environmental studies [4-5]. GEP has been employed in this study (i.e. determination of stability constants) because of its linear Nernstian response, rapid reversibility and high sensitivity to aqueous hydrogen ions over a wide concentration range [5]. However the accuracy of the results from (GEP) depends on the calibration procedure of the electrode employed in a particular study [5-7]. The measuring setup for potentiometric measurements always consist of two electrodes, a measuring or indicator electrode and a reference electrode. For practical reasons these two electrodes are usually contained in a single combined glass probe/electrode; as illustrated by Figure 2.1 below.

The reference electrode (usually Ag/AgCl) is an oxidation/reduction half cell of known and constant potential at a particular temperature, which is independent of the sample solution (reference potential) [5]. From the reaction cell, the observed potential(i.e. E_{cell}) is due to the

individual potentials from the reference E_{ref} , indicator electrode E_{in} and liquid junction potential E_g. This is represented by the following equation;

$E_{cell} = E_{in} + E_{ref} + E_g$

The potential measurement itself takes place virtually current free in the presence of a volt-meter, with a high impedance measuring input to avoid any potential drops during the analysis [5].

Figure 2.1: schematic diagram of a combined pH glass electrode dipped in solution

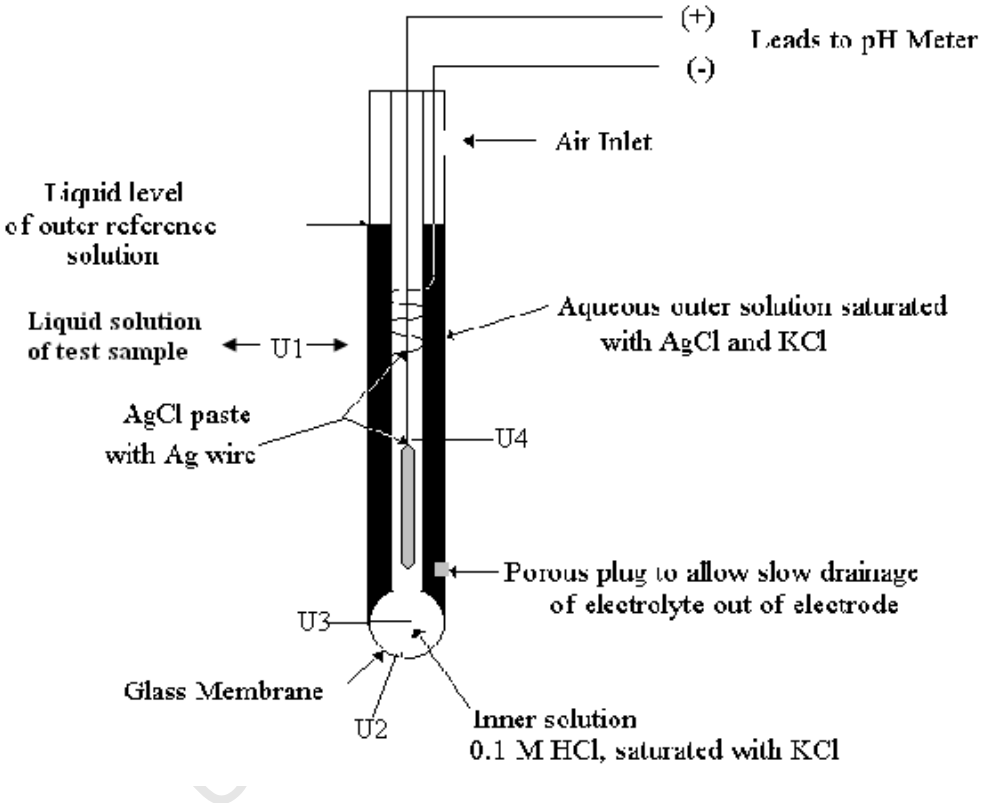

Where:

U1: Galvani potential between measuring electrode and measuring solution
U2: Galvani potential between internal buffer and glass membrane
U3: Galvani potential between internal reference electrode and internal buffer
U4: Galvani potential of reference electrode
U5: Diffusion potential at the diaphragm

The indicator electrode (in this case a pH glass electrode) produces a potential E_{cell} (relative to the inert reference electrode), which is dependent on the sample solution (i.e. is proportional to the logarithm of the analyte activity {H}).

The hydrogen ion activity is obtained from the emf reading of the glass electrode, following Nernst equation:

$$E_{cell} = E_r + E_i + E^o_g + RT/F * \ln \{H^+\} \quad (2.2.15)$$

Where: E_{cell}= the measured emf of the cell

E_r = contribution arising from the reference electrode

E_i = contribution arising from the liquid junction

E_g = standard glass-electrode potential at unit activity

R =universal gas constant

T = absolute temperature

F = Faraday constant

{H} = hydrogen ion activity

For the quantitative evaluation of data the Nernst equation is used to convert the experimental electromotive force values (E) into the equilibrium hydrogen ion concentration [H]. This is the case because the activity {H} of the hydrogen ion is defined as constant in solution with a constant ionic strength [4].

Ionic strength of a solution is defined by the following expression;

$$I = \tfrac{1}{2} \sum C_i Z_i \quad (2.2.16)$$

Where C_i is the concentration of ionic species i and Z_i is the charge on that ion.

If the ionic strength is kept constant, the hydrogen ion activity can be expressed as a concentration, this concept of ionic strength was first introduced by Lewis and Randall in 1921, who stated that in a dilute solution, the activity coefficient of a given strong electrolyte is the same in all solutions of the same ionic strength [6] and equation 2.2.15 can be obtained by setting s (i.e. slope) = 2.303RT/F and collecting together all the constants as E_{const}:

$$E_{cell} = E_{const} + s\log [H] \quad (2.2.17)$$

Furthermore it is interesting to note that the slope (i.e. s) of the Nernst equation indicates the temperature dependence of the measured cell potential.

2.4 Factors affecting the stability constants of complexes

Complex formation is defined as the association of two or more simple species, each capable of independent existence [3, 6]. Therefore as a result, many species may form in solution and only the stability constants of the major species formed are used to select/describe the chemical speciation occurring in solution [6].

The strength of the complex formed in solution is better described in terms of the Pearson's hard/soft-acid/base theory, HSAB, in which an acid or base is classified as either hard or soft or intermediate between the two [6]. According to this theory a hard acid will prefer to bond to a hard base while a soft acid will prefer to bind to a soft base [6]. More recently it has been suggested that a steric component plays a major role in the observed HSAB behaviour in solution, in addition to the covalent and ionic contributions [5-6, 10].

It is a fairly general observation that the equilibrium constants of analogous complexes involving divalent-metal ions Mn through Zn and ligands that contain nitrogen as donor atoms; examples include ethane-1, 2-diamine (en), follow the order: $Mn^{+2} < Fe^{+2} < Co^{+2} < Ni^{+2} < Cu^{+2} > Zn^{+2}$, which is referred to as Irving-Williams order\series [6-7]. However there may be some alteration in the series, this is thought to be caused by a change in the electron distribution on the metal ion centre (i.e. high spin to low spin or vice versa) [7]. A stable complex is one with its ligands spread around the metal ion in such a way as to minimize repulsion. Many metal ions also have bond directionality and in these special cases the positions of the ligand around the metal ions play a major role in the resulting complex stability [8].

2.4.1. Chelate effect

There is a pronounced increase in the formation constant of metal complexes containing a bidentate ligand as compared to monodentate ligand containing complexes [8-9]. This enhanced stability is referred to as the chelate effect which is entropy driven [8]. The chelate effect is

dependent on the size of chelate ring, with 5-membered and 6-membered chelate rings being the most stable, [4, 6-8]. It was also found that the stability of the complexes of divalent metals ions with the macrocyclic ligand is greater when compared to the complex with the analogous open-chain ligands [6]. This phenomenon is referred to as the macrocyclic effect. Perhaps the marked differerence between macro-cyclic ligands and open chain (chelating) ligands, is their selectivity for metal ions, based on the metal ion fitting perfectly (i.e. at optimal distance and geometry) from the donor groups in the cavity of ligand. This leads to two important factors which contribute to the stability of macrocyclic-metal complexes. These are the preorganisation of macrocycle (enthalpy effect) and the size of the chelate rings (entropy effect).

In order to understand these two effects we must invoke two well known thermodynamic relationships:

$$\Delta G^{o} = -R\,T\,\log K \qquad (2.2.13)$$

$$\Delta G^{\circ} = \Delta H^{\circ} - T\Delta S^{\circ} \qquad (2.2.14)$$

Where: ΔG° is the standard Gibbs free energy, R =universal gas constant, T = absolute temperature, ΔH° is the standard enthalpy and ΔS° is the standard entropy.

These two parameters can be calculated by either using the Vant' Hoff equation, or calorimetry, with the latter been favoured for practical reasons. Enthalpy effects depend on bond strengths and entropy effects referrer to the changes in the order/disorder of the solution as a whole [6]. Preorganization in macrocyclic ligands is based on a principle that the free ligand has less entropy relative to an open chain chelater because of its limited conformational states and hence the change in entropy upon metal ion coordination is less [8]. There is also an enthalpy contribution because, in a flexible ligand, the free ligand would need to adopt a higher energy conformational state before coordination can occur. In the pre-organized ligand, this increased energy has been built into the molecule during synthesis [8].

2.5 Data analysis

Even with the current development of highly non-invasive techniques for the determination of stability constants, considerable discrepancies continue to exist between the values published for the same chemical system by different authors [5-10]. This commonly occurring phenomenon was concluded as being associated with the computer analysis of the titration data employed by these researchers, the most likely source of error being 'choosing the correct model' to explain the chemical system [9]. In this study we have used the ESTA suit of programs to analyse the data.

2.5.1 The ESTA (Equilibrium Simulation of Titration Analysis) Program Library.

Computer analysis of equilibrium data has replaced the graphical methods used in the past, and many programs exits to analyse potentiometric data (Martell and Motekaitis, 1988). One such program is ESTA, which was intended as a flexible tool for the determination of protonation and formation constants in aqueous chemical equilibria. The program library is used to calculate equilibrium distributions of chemical species, to analyse potentiometric titration data and to manipulate titration data for a variety of other purposes. The calculations are performed using a Gauss-Newton method to solve the mass balance equations (m.b.e) which were discussed in section 2.2.

At each point of the titration the computer calculates the emf of the system and finds the difference between the calculated and the observed values. The difference is then squared and summed to give a value of U, the object function, given by

$$U = (N-n_p)^{-1} \sum n_e^{-1} \sum w_{ni} (Y_{ni}^{obs} - Y_{ni}^{calc})^2 \qquad (2.3.1)$$

Where

N = total number of experimental titration points

n_e = total number of electrode (one in this study)

n_p = is the total number of parameters being optimised

W_{ni} = weight of i^{th} residual at n^{th} point

Y_{ni} = total concentration of electrode ion i or the electrode emf of electrode i, at the nth titration point.

In order to minimize U, a gauss-Newton approach is employed and this assumes that the function is quadratic with respect to all the parameters. Therefore U can be expressed as;

$$U = a + p^t b + (p^t H p)/2 \qquad (2.3.2)$$

Where a and b, are the Gauss-Newton quadratic parameter vectors, p is the optimization parameter vector, p^t transpose of p and H, the Hessian, is given by:

$$H_{sr} = d^2U/dp_{spr} \qquad (2.3.3)$$

A well defined system, with good initial estimates, often converges. Calculations are terminated if the shift vectors are large or if the shift vector has an upward gradient. This indicates that there was something wrong with the input data and therefore the mass balance equation cannot be solved [3].

Once U is sufficiently minimized, the standard deviation, the Hamilton R-factor and its limit are reported together with the optimised values of the stability constants.

The Hamilton R-factor (R_f) and the R-limit (R_{lim}) are calculated using the following formulae:

$$R^f = [U / \Sigma n_e^{-1} \Sigma w_{ni} (y_{ni}^{obs})^2]1/2 \qquad (2.3.4)$$

$$R_{lim} = [N/\Sigma n_e^{-1} \Sigma w_{ni} (y_{ni}^{obs})^2]1/2 \qquad (2.3.5)$$

ESTA is also used to calculate two important functions from the titration data, and are explained below.

2.5.2 The Formation Function (Z-bar) and Deprotonation Function (Q-bar)

In the absence of a metal ion, the formation function (Z_H) is expressed as;

$$Z_H = (T_{*H} - H + OH)/ T_L \qquad (2.3.6)$$

Where T_{*H} is the total hydrogen ion concentration, T_L is the total ligand concentration and

$OH = K_W/ [H]$. Z_H can also be defined as the average number of hydrogen ions bound to the ligand at each pH reading. The Z_H is plotted against pH.

In the presence of a metal ion, the formation function (Z_M), is expressed by;

$$Z_M = (T_L – [L])/T_M \quad (2.3.7)$$

Where T_L and T_M are the total concentration of the ligand and metal respectively, and [L] is the free-ligand concentration. T_L is given by equation 2.3.6. And also Z_M is also plotted against pL or (-log [L]).

However this definition of the complexation function (Z_M), only applies to mononuclear binary complexes. A plot of Z_M-bar-log [L], gives a picture of the representative species in equilibria. If only simple, mononuclear, binary species are formed in solution, then the graphs determined from titrations performed at deferent initial ligand, and metal concentrations should overlap one another through the pH range of interest. If this does not happen then this means that there are other species formed in solution. The mysterious fanning back of the Z_M-bar curves indicates the presence of hydroxo or mixed hydroxo species [7]. This behaviour by the graph can assist in choosing the correct model for description of an unknown chemical system and hence for the refinement process (discussed later, see section 2.6.5).

The deprotonation function (Q-bar), is defined as the average number of protons released per metal ion upon complexation with the ligand, and is expressed as follows;

$$Q_M = (T_{H^*} - T_H)/T_M \quad (2.3.8)$$

Where T_H and T_M are the total hydrogen ion and metal concentrations respectively

T_{H^*} is the calculated total concentration of the protons that would be necessary to give rise to the observed pH if no complexation took place, is given by the following equation;

$$T_{H^*} = [H] – [OH] + \Sigma r\beta_{pqr}[L]^q[H]^r \quad (2.3.9)$$

Where, the summation is over all protonated ligand species.

In a binary system, a formation function represents the number of protons that would be on the ligand in the absence of the metal ion, and is given by the following equation;

$n_H = (T_{H^*} - [H] + [OH])/T_L$ (2.3.10)

The difference (r) between n_H and Q-bar gives the number of protons on the metal complex. This can be represented as;

$r = (q \times n_H) - (Q_H \times p)$ (2.3.11)

Where, p and q are the stoichiometric coefficients of the metal and the ligand respectively.

2.5.3 Data error analysis

In any physical measurement, knowledge of the errors involved is important. A typical example is thermodynamic data where good protononation and stability constants require minimal experimental errors on the part of the researcher. Identification of experimental error can be done by studying a well known system for instrumentally generated errors, or by varying the reaction conditions for a particular system and observing its reproducibility. Random errors in the experimental data are reduced by an increase in the number of titrations and titration points.

2.5.4. Weighting.

Weighting is a very important part of analysing data for errors. This is because, while the error maybe constant, the information content and hence importance of each data point is not. By weighting each data point according to its informational content, the influence of experimental (random) error can be minimised. There are many other benefits, including (a) a more practical approach for dealing with changes in conditions such as temperature and ionic strength and (b) a more objective method of reconciling the marked differences that often occur between published parameters from independent investigators, thus the data can aspire to both be critical and comprehensive [5]. Weighting is defined as the reciprocal of the variance of the residual between the real and the calculated and the weight(p) of the i^{th} residual at the n^{th} point is given by the following expression;

$Wni = [\Sigma (d (y^{obs}_{ni} - y^{calc}_{ni})/dp)^2 \sigma^2 p]^{-1}$ (2.3.17)

Where, y^{obs}_{ni} and y^{calc}_{ni} are the observed and calculated variables of q^{th} residual at nth point respectively. σ_p is the standard deviation in the parameter p to be optimised.

Experimental

2.6 Equipment

All titrations were performed in an inert double-walled reaction vessel maintained at 25ºC by a steady flow of water from the thermo-stated water bath using a Metrohm 799 GPT Titrino equipped with automatic burette and a Metrohm combined glass electrode system (i.e. pH/mV meter). The slope of the electrode system was calibrated in terms of hydrogen ion activity using buffer solutions of known pH's and E_{const} was determined by strong acid - strong base titrations at 25 ºC. The 799 GPT Titrino is also further equipped with an internal data chip programmed for equilibrium aliquot titration and titration data recording, thus controls all the functions of the burette without the need of a computer. The reaction medium was kept inert by a steady gas flow of pure humidified inert nitrogen gas. The nitrogen gas was purified before going into the reaction vessel by bubbling it through different glass bottles containing, 50% potassium hydroxide to remove carbon dioxide, Fierser's solution to remove oxygen, glass wool, distilled water and finally the gas is passed through a solution of background electrolyte solution of ionic strength 0.15 M NaCl.

2.6.1 Preparation and standardisation of solution

All solutions were prepared with recrystallized NaCl (Fluka) as background electrolyte, at ionic strength of 0.15 mol/dm^3 (Cl^-)Na^+ in double glass boiled distilled water. The water is double glass boiled to remove the trapped CO_2 and is finally kept in a plastic container (polyethylene bottle) protected by a carbosorb (sodium carbonate pellets) or CO_2 trap. All reagents were commercially available and of analytical grade. These were used without further purification. However PCU.homopiperazine was obtained from the University of KwaZulu Natal, in a yellow oil form.

The solution of HCl was prepared to a concentration of 0.01 mol dm^{-3} from Merck ampoules (1.09959 – Titrisol) in sufficient sodium chloride to give the ionic strength of 0.15mol.dm^{-3}. The

solution was standardised against recrystallized sodium tetraborate decahydrate (borax) $Na_2B_4O_7 \cdot 10H_2O$.

The solution of 0.0995 M NaOH was prepared under nitrogen atmosphere from Merck ampoules (1.09959-Titrisol). The resulting solution was standardised with a primary standard Potassium hydrogen phthalate (KHP) which was dried over night in an oven set 110 ◦C before use. NaOH solution was further standardised against 0.01 M HCl solutions.

2.6.2 Preparation of Ligand solutions

Stock solution of each ligand (i.e. homopiperazine and PCU.homopiperazine) was prepared to a concentration of 1.0 mM and 7.6 mM respectively. Each ligand solution was prepared by accurately weighing the exact mass required of each in a 100ml volumetric flask and diluting to the mark with a standard solution of HCl. Both ligand solutions were corrected for ionic strength by adding sufficient sodium chloride as background electrolyte. Standardization of each ligand was performed by acid – base titrations according to Gran's method [14, 15],

Addition of 0.01 M HCl resulted in the pH of the ligand solution dropping to a value of 2 and this was done in order to increase the solubility of ligand and to make sure that the ligand was fully protonated [15, 21].

2.6.3. Preparation of metal solutions

Standard solutions of divalent cations Cu(II) and Zn(II) were prepared from $CuCl_2 . 2H_2O$, and $ZnCl_2$ respectively and similarly as above, the solutions were corrected for ionic strength by adding background electrolyte. Each metal solution was standardised by direct titration against 0.01 M standard solution of disodium salt of ethylenediamine tetraacetic acid (Na_2EDTA) using standard methods [13, 15]. Fast sulphon black F (FSB) and solochrome black (SB) were used as indicators for the determination of Cu^{+2} and Zn^{+2} ions respectively. Furthermore prior to the direct titration with Na_2EDTA, all divalent metal ion stock solutions were purged overnight with a small portion of acid (i.e. 0.01 M HCl) and this was done to reduce metal ion hydrolysis and the

subsequent metal hydroxide precipitation, which may lead to a the wrong metal concentration determined in solution. The metal ion concentrations were in the range between 0.01-0.0087 $mol.dm^{-3}$.

2.6.4. Equipment and Titration procedure

Before any electrode calibration could be done the electrode was stored over night in a 0.01 mol/dm^3 HCl solution, this was done to improve the response of the electrode. The slope of the glass electrode was calibrated for hydrogen ion activity with commercially available buffer solutions of known pH (i.e. 4, 7.02 and 9.18) done according to Vogel's procedure [13]. The Nernstian slope was accepted if it fell in the range 58.60 — 59.16.

The pKw (i.e. the dissociation constant of water), the E_{const} and slope (s) of the electrode were calibrated using an acid-base titration. For a more precise data analysis of these electrode parameters, the titration data was imported into the ESTA file template. Furthermore only titration data in the pH region of 2.3-2.9 and between 10.8 and 11.3 were used. This was done to reduce the effects caused by liquid junction potential, acid error and to minimize sodium errors found at high pH values respectively. The electrode calibration using acid-base titration was performed to suit the conditions such as temperature (25ºC) and ionic strength (I= 0.15 mol/dm^3) [15].

The ligand protonation titrations were performed by directly weighing appropriate aliquots of the stock ligand solutions into the reaction vessel. This solution was then titrated against the standardised NaOH solution introduced via piston burettes at preset volume increments into the titration cell maintained at 25 $^{\circ}$C. In one trial titration the (mV/pH v/s burette volume), data is recorded at each point (i.e. each volume increment) and is examined until equilibrium is reached. This together with accurate knowledge of base concentration, total acid concentration, pKw and electrode parameters (i.e. E_{const} and electrode slope), allows for the determination of protonation constants in ESTA (discussed later). Addition of NaOH solution does not change the ionic strength of solution, because the measurements are performed starting from fully protonated

polyamines, so each $-NH_x^+$ cation will be replaced by equivalent amounts of Na^+ ions [5]. The same procedure was carried out for the metal-ligand complexometric titration but with initial varying concentrations ratio of the metal ion and ligand. All solutions except the ligand (which was weighed) were introduced via piston burettes, read to precision of 0.03 ml. All titrations were performed in duplicate, and were constantly stirred by a magnetic stirrer.

The metal complex formation curves were obtained at 2:1 to 3:1 ligand to metals ratio. However for both Zn(II)–HP and Zn(II)-PCU-homo systems precipitated or the Zn(II)-hydroxide was formed as pH was increased >7. This limited our analysis for stability constants for the Zn(II)-PCU-homo complexes.

2.6.5 Experimental Data Analysis

Data analysis was done with the help of ESTA (Equilibrium Simulation for Titration Analysis) computer library. Prior to data analysis the guessed complex species and their stability constants were calculated using the task BETA of the ESTA program. These were then entered into a preformatted ESTA data file for the determination of protonation constants and using task OBJE in the ESTA2A module, which gave out modified values of the stability constants. The OBJE task was also used to optimize for the weak acid or ligand concentration describing the system. While for the determination of metal complex formation constant, the titration data was imported into a preformatted ESTA data file for the determination of metal complex stability constant which also contains metal hydrolysis constants obtained from data of Baes and Mesmer and Krateng at 25ºC which have been corrected for ionic strength I= 0.15 M [12]. Then the thermodynamic parameters (i.e. metal complex formation constants β_{pqr}) were calculated the same way as protonation. The reported formation constant results are based on a correct model determined using complex formation function (Z-bar) calculated in the ESTA1 module. Furthermore, from the experimental data the models were accepted as correct when the observed and calculated plots of Z_H-bar, and Z_M-bar overlapped each other respectively and output data giving acceptable values of standard deviation and Hamilton R-factors. The species distribution

graphs were obtained by substituting the final stability constants into the SPEC task in ESTA and the plots were obtained by using plot 1 option in SPEC.

Task SPEC was then finally used to calculate the species distribution diagrams as a function of pH and further used as a criterion to check the validity of the model chosen to explain the system. The study of homopiperazine system was studied in order to check the experimental procedure. The results shown in table 2.1 were in good agreement with the values reported in literature for a similar system.

2.7 Results and Discussion

2.7.1 Protonation Constants

The overall protonation constants (log β_{pqr}) for the homopiperazine system were investigated in the pH range 2-11. These protonation constants were confirmed by a complete overlap of the calculated (theoretical) and the observed Z_H-bar curves, shown in Figure 2.2(a). The values of the protonation constants (log β_{pqr}) for the homopiperazine are given in table 1.

2.7.1.1 H^+-homopiperazine system

Figure 2.2(a) protonation formation curve, Z_H-bar plotted against pH for homopiperazine at 25° C in 0.15 M $Na^+(Cl^{-1})$. The different symbols in the graph represent titrations performed at different initial concentrations, and the solid line is the theoretical curve calculated using the model in Table 1.1. (b) Protonation species percentage distribution curves of homopiperazine ($[L]_T$=1.0mM) as a function of pH.

(a) (b)

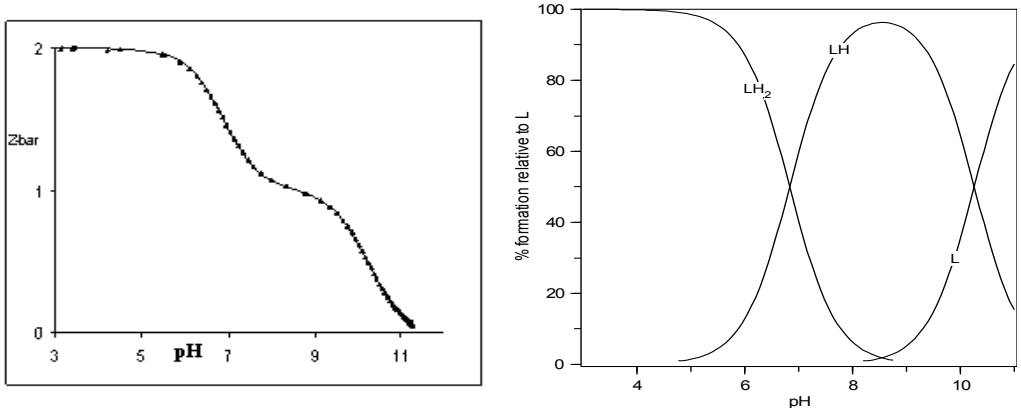

Figure 2.2(a) shows the average number of protons on homopiperazine (HP), i.e. Z_H-bar, as a function of pH. The Z_H-bar function rises and levels off on 1 (i.e. Z_H-bar= 1) at pH 10. This indicates that one amine group in the HP system is protonated. Furthermore the Z_H-bar function then rises again and plateaus when it reaches a value of 2 at pH 7, thus indicating the simple stepwise protonation of the second basic site. This indicated that, there are 2 protons bound to the ligand, with pK_a values of approximately 10 and 7 respectively. The final refined equilibrium constant values with their corresponding standard errors are given in Table 1. The agreement between the observed and calculated formation curves (see Figure 2.2(a)) and the low standard deviations in the refined pronotation constants give more confidence in the results (see Table 1).

The calculated speciation diagrams (i.e. calculated for 1 mM solution) of homopiperazine based on the stability constants reported in Table 1.1, is shown in Figure 2.2(b). From this diagram it is clear that, between pH's 2 and 7.1, the LH_2 species is present as the dominant species, reaching approximately 98%. LH only starts forming at pH 7.6, with the neutral species (i.e. free ligand [L]) only reaching significant amounts in solution when the pH>10.

Table 1.: $\log\beta_{pqr}$ of homopiperazine and Cu(II)-homopiperazine system determined at 25 ºC in 0.15 mol/dm^3 (Cl^-) Na^+. S.dev denotes standard deviation in $\log\beta_{pqr}$; R_f^H is the Hamilton R-factor and $R_{lim}H$ its limit. n_t is the number of titration points. The general formula of a complex is $M_pL_qH_r$ denoted by the stoichiometric coefficient pqr.

LIGANDS	p q r	s.dev	log β	R_{lim}^H	R_f^H	n_t	Lit [18]
HP-H_n^+	0 1 1	0.002	10.21	0.01	0.008	136	10.26
	0 1 2	0.003	17.09				16.6
HP-Cu(II)	1 1 0	0.01	7.6	0.03	0.02	600	7.8
	1 2 0	0.01	12.6				13.8
	1 1 -1	0.03	1.88				

The pK_a values obtained for homopiperazine agree well with those from the literature (see Table 1). The pK_1 of 1, 3-diazacyclohepane (homopiperazine) is 0.77 log units greater than that of a related derivative piperazine (pK_1 9.44). This phenomenon is believed to be caused by the positive inductive effect of the extra methylene group on homopiperazine.

There is also a slight increase in the pK_2 of HP due to the increased inter-nuclear distance between the two amines which results in less repulsion experienced between the two amino groups. A similar trend of an increase in base strength brought about by methyl substitution is also reported by Golgberg *et al.* [16] in a series involving ethylenediamine and its substitution products, N-methylethylenediamine, N'N''-dimethylethylenediamine, $pK_2 = 6.63$, $pK_2 = 9.90$; $pK_2 = 10.2$ respectively. The relatively low pK_2 value for the second protonation site compared to the first (pK_1) in HP is due to the columbic repulsion between the incoming proton and the proton already attached to the ligand [10-16]. Statistical factors must also play a role as the stability constants decrease with decreasing number of available binding sites on the ligand [6-8, 14]. The pK_1 of homopiperazine was observed to be 0.43 log units less than the pK_1 (10.64) of methyl amine [10]. This is expected in moving from primary to secondary amines due to steric hindrance and solvation effects which are reported to override the positive inductive effects in molecules [10-15]. Furthermore pK_1 of homopiperazine is quite similar to the pK_1 10.16 reported by E. Bianchini *et al*. [20] for a related secondary amine derivative N', N''-diethylethylenediamine despite a different background electrolyte being used, thus giving further confidence in the values of the protonation constants obtained.

2.7.1.3 Cu(II)-homopiperazine system

The formation function (Z_M-bar) and complex species percentage distribution curves of the Cu(II)-homopiperazine system are shown in Figures 2.3(a) and 2.3(b) respectively.

The complex formation function, Z_M-bar, measures the average number of ligands bound per metal ion. This function is plotted against the negative logarithm of free ligand concentration (pL).

Figure 2.3(a): formation function curve, Z_M-bar against pL for homopiperazine at 25 ºC in 0.15 M NaCl. The symbols represent complexation curves for various metals to ligand ratios, [(▄) 1:1, (▲) 1:2 and (●) 1:3) and the theoretical curve is the solid line. (b) Complex species percentage distribution curves of homopiperazine-copper system (1:2 ratio) as a function of pH

(a) (b)

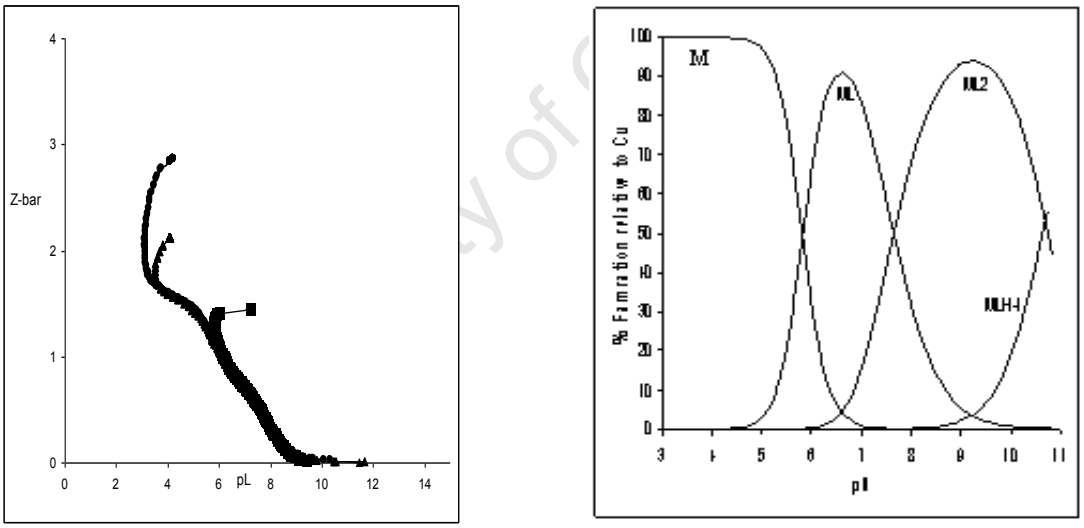

Figure 2.3(a) shows the Z_M-bar function for Cu(II)-homopiperazine system plotted against pL. At high pL (i.e. low free ligand concentration) or high pH the Z_M-bar-function rises and slightly plateaus below 1. This indicates the stepwise complexation of one ligand to a single divalent copper ion, therefore forming the ML species at pH 7.5. As pL decreases, the curves rises again and plateaus at 1.7 at pL 4.7, thus indicating the attachment of the second ligand to the metal ion and formation of ML_2. At different metal:ligand ratios the curves are super-imposable indicating

formation of a mononuclear complex as the major species formed in solution. However, at higher pH the Z_M-bar curves 'fan-back', thus indicating the formation/presence of a hydroxo species in solution.

Analysis of the data yielded the model presented in Table 1.1. An excellent agreement between the theoretical (i.e. solid line) and experimental complex formation curves in Figure 2.3(a) at different metal to ligand ratios further supported the model chosen in the data analysis. The model showed a reasonably low R factor and relatively small standard deviations in the log β_{pqr}s, thus giving confidence to the model chosen. Comparing the formation constants (7.6) in Table 1.1 for the ML species, with (β_{110} = 8.34) for (N, N'-dimethyltrimethylene-1, 3- diamine reported by T.A. Kaden *et al*. [8], it is interesting to note that HP forms a weaker complex with copper (II). However this is expected because of the weak base strength (i.e. low pK_a values) exhibited by the amines in the homopiperazine system. Furthermore in comparing the formation constant of homopiperazine with of N', N''-dimethylethylene-1, 3-diamine [17] (β_{110} = 9.95), the ML species of the latter is more stable than the ML species for copper (II)-HP system. This is the case despite N'N''-dimethylenethylene-1, 3-diamine having a slightly lower base strength. Perhaps the reason for the weak complex might be from the ring strain in the case of homopiperazine (i.e. no freedom for rotation around the C-N-C bond in homopiperazine when compared to its linear analogue) [10]. Also the fact that homopiperazine forms 6, 5 membered chelate rings at the same time upon metal binding while in the case of N'N-dimethylethylene-1, 3-diamine only a single 5 membered chelate ring is formed may account for the weak complex strength.

Comparing the equilibrium constants of ML (7.6) and ML_2 (5) for HP-Cu (II) system, there is as considerable decrease in complex stability in moving from ML to ML_2 and this is consistent with and can be attributed to steric crowding around the metal ion as more donor groups are involved in the formation of ML_2 when compared to the two amines in ML species [14-17]. From the species distribution curve in Figure 2.3(b), calculated from the data in Table 1.1, it is clear that complexation starts at pH 4.5 with the formation of ML species, while MLH_{-1} only starts forming

at higher pH values. It is interesting to note, from Figures 2.3(b) that as the ratio of ligand: metal is increased the onset of MLH_{-1} formation is suppressed. Furthermore ML_2 is the dominant species in physiological pH 8-9 range reaching close to 90%.

2.7.2. PCU.homopiperazine system

The formation and stability constants were evaluated using a similar procedure that was employed in the investigation of the HP system.

2.7.2.1 Protonation constants

The ligand PCU.homo possesses two secondary and two tertiary amines, so as expected, the ligand was able to take-up four protons (see Figure 2.4 (a)). Table 2.2 contains the logarithm of the overall protonation constants for the studied ligand. In the pH range of interest (2-11), PCU.homo presents two of its secondary amines as moderate to strong bases with the remaining amines behaving as weak bases. This trend is consistent with many reported protonation sequences of polyamine systems [14].

2.7.2.2 H^+-PCU.homo system

Figure 2.4(a): protonation formation curve, Z_H-bar plotted against pH for PCU.homopiperazine at 25 ºC in 0.15 M NaCl. The symbols represent titrations performed at different initial concentrations, while the solid theoretical line was calculated using the model given in Table 2. (b) Protonation species percentage distribution curves of PCU.Homopiperazine ($[L]_T$=7.6mM) as a function of pH.

(a) (b)

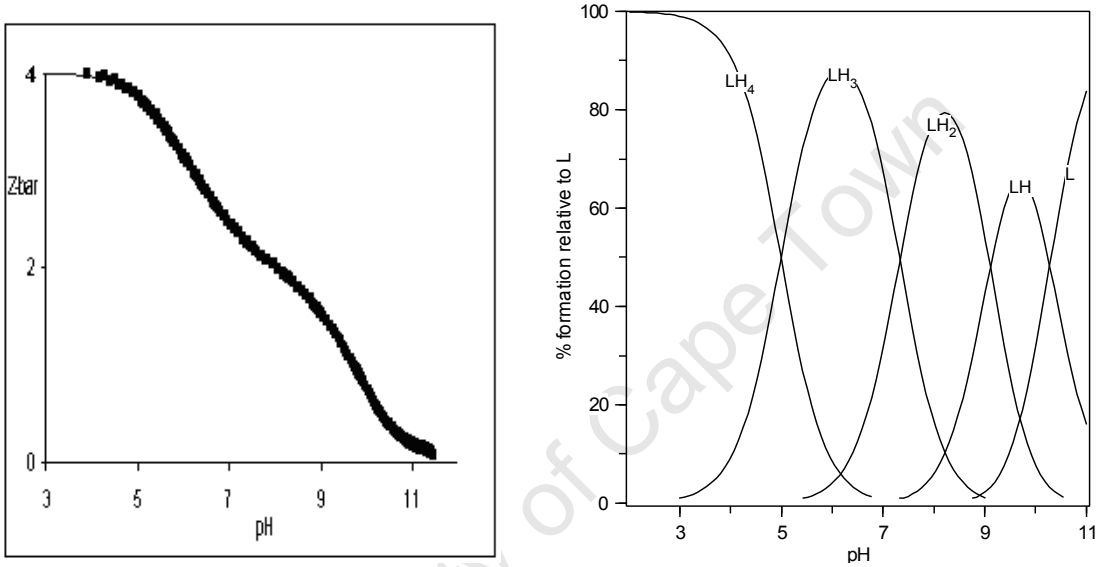

Figure 2.4(a), shows the protonation function (Z_H-bar) as a function of pH. At high pH (> 11) the curve is at zero (i.e Z_H-bar = 0) indicating that the last proton is lost from the ligand, this is also confirmend in the species protonation distribution curve (see Figure 2.4(b) with L being dominant species at higher pH's (> 10). As the pH decreases, the Z-bar rises again and levels slightly below 2 (i.e Z_H-bar = 1.8) at pH 7, indicating that there are two protons added on the ligand. Note there is no leveling off of the curve at Z-bar 1 indicating that pK_{a1} and pK_{a2} are very similar. Between pH 7 and 5 the curve rises further and plateaus at a Z_H-bar value of 4 indicating that a further two protons have been added to the ligand.

Analysis of the experimental data yielded the proposed model in Table 2, comprising of the following four species LH, LH_2, LH_3 and LH_4 and these were then used to explain the protonation sequence. From Figure 2.4(a) the leveling off of the Z_H-bar curve between pH 9 and 7 at 2, indicates that the di-protonated species LH_2 will be dominant over the physiological pH range. This is cornfirmed by the calculated species distribution graph in Figure 2.4(b) which indicates the presence of LH_2 as the dominant species in the physiological pH range of 7 to 9 reaching 87%.

Another interesting and noticeable feature in the graph is that the initial rise of the Z-bar function to a value of 2 indicates that two protons are added simultaneously (i.e. have similar pKa values) [20]. This trend has also been observed for related tetra-amine system, {3,7,15,19, 25, 26-hexaazatricyclo[19.3.1.1]hexacosa-1(25),9,11,13(26),21,23-hexane} reported by Dhont *et al*. [21].

Table 2: $\log\beta_{pqr}$ of PCU.homopiperazine system determined at 25 ºC in 0.15 mol/ dm^3 (Cl^-) Na^+. S.dev denotes standard deviation in $\log\beta_{pqr}$; R_f^H is the Hamilton R-$_{factor}$ and $R_{lim}{}^H$ its limit. n is the number of titration points. The general formula of a complex is $M_pL_qH_r$ denoted by the stoichiometric coefficient pqr.

LIGANDS	p q r	log β	pK_a	S.dev	R_{lim}	R_f^H
PCU.homo-H_n^+	0 1 1	10.28	10.28	0.01	0.006	0.01
	0 1 2	19.39	9.11	0.01		
	0 1 3	26.27	6.88	0.01		
	0 1 4	31.71	5.44	0.02		

Table (2) shows the protonation constants for PCU.homo together with their corresponding statistics. A low R-factor further indicates the correctness of the protonation model chosen and thus increases the confidence in the values obtained experimentally. It is interesting to note that the pK_1 of PCU.homo is only 0.02 log units higher than pK_1 (10.26) for homopiperazine, thus

suggesting that the cage structure has little effect on the pK_1 of PCU.homo. As can be noticed from the speciation diagram (i.e. Figure 2.4(b)), at the start of the titration LH_4 is the dominant species at 95%, this also gave further support that the model chosen to describe the protonation sequence for the system of PCU.homo is correct.

The difference in the pK_a between pK_1(10.28) and pK_2 (9.11) is 1.17 log units, and this suggests that the binding of first and the second proton are independent of each other. However this decrease in basicity, indicates that protonation of the second amine group is slightly more difficult. This is thought to be as a result of repulsion between the incoming proton and the proton already attached to the ligand or this phenomenon can be explained as caused by a statistical factor following the well established thermodynamic fact that stability constants decrease with decreasing number of available binding sites. Comparing the $\Delta pK_{1,2}$ in HP (i.e. $\Delta pK_{1,2} = 7$) and that of PCU.homo (i.e. $\Delta pK_{1,2} = 1.17$), this implies that the first two protonation process in PCU.homo system is occurring on nitrogen atoms that are separated by at least four methylene groups and consequently, these two protons should be located at the terminal amines, and this is shown in the proposed protonation scheme (i.e. K_1 and K_2) in Figure 2.5 below.

The two low protonation constants pK_3 and pK_4 (i.e. 6.88 and 5.44 respectively) correspond to the protonation of the tertiary amines connected to the rigid cage through an alkyl group.

The difference in the pK_3 and pK_1 is 3.4 log units. This decrease in the third pK_3 is as a result of the electrostatic repulsion on the ligand caused by the two protons already bound to the terminal amines, thus introducing a negative inductive effect on the whole molecule [20, 21]. Furthermore pK_3 (6.88) of PCU.homo is 0.18 log units lower than the pK_3 (7.06) of PCU.EN (N, N'-bis [ethylene diamine]-4-[oxahexacyclododecane]) a related penta-cycloundecane derivative [21]. This low pK_3 value observed for PCU.homo relative to PCU.EN can be explained by solvation effects caused by the extra steric crowding around the tertiary amine. This decrease in amine basicity has also been reported when a secondary amine is methylated [10]. It is interesting to note that PCU.homo exhibits a more basic terminal secondary amine than the terminal primary

amine of a related penta-cycloundecane ligand (PCUA), with $pK_1 = 10.26$ and $pK_2 = 9.517$ respectively reported by Jackson *et al*. This is because the primary amines in PCUA have their base strength weakened by the effect of the CONH group [20].

Figure 2.5: Protonation scheme for PCU.homopiperazine. The cage moety was been removed for clarity.

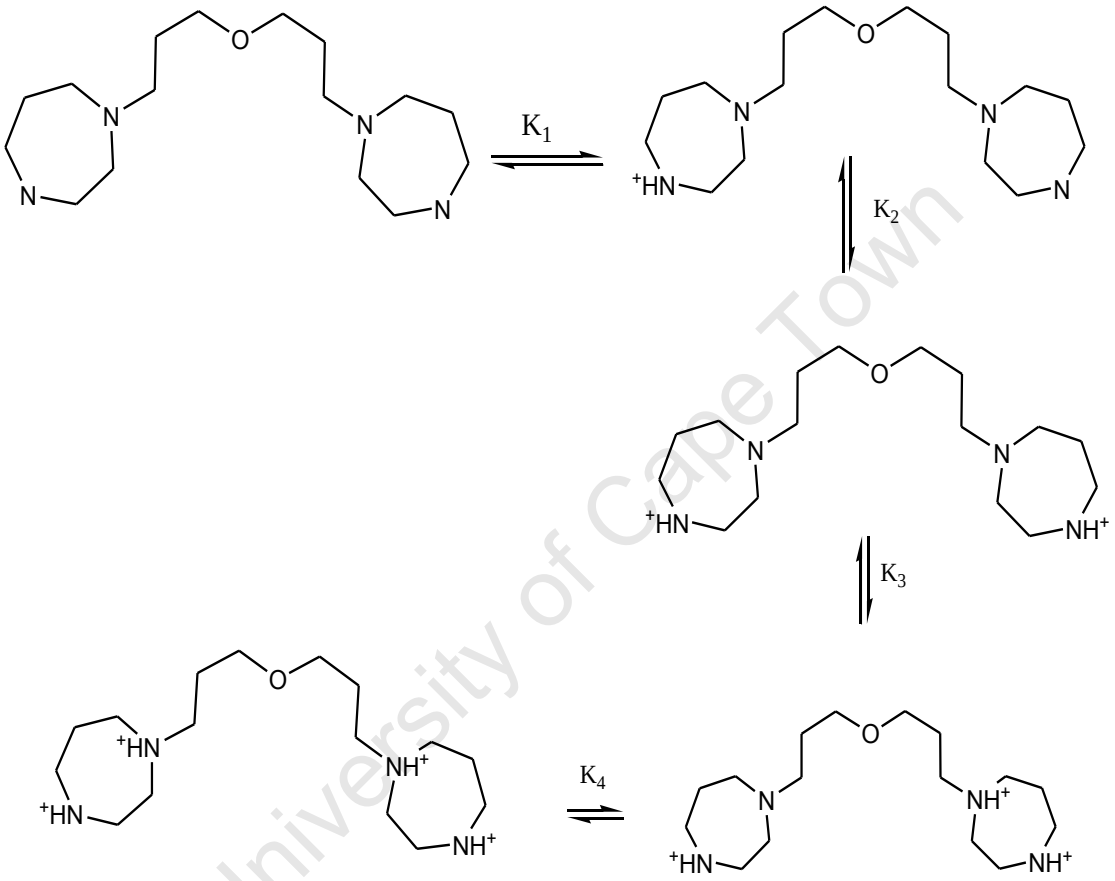

2.7.2.3 Complex formation

The stability constants were evaluated and confirmed in the same way as mentioned above in the pH range of interest 2-11 and results are listed in Table 2.2 below.

2.7.2.3.1 Cu(II)-[PCU.homopiperazine] system

Figure 2.6: (a) Formation function curve, Z_M-bar against pL for PCU.homopiperazine-Cu(II) at 25ºc in 0.15 M Na^+ (Cl^-). The symbols represent complexation curves for various metals to ligand ratios, [(▄) 1:3, and (▲) 1:2, while the solid theoretical line was calculated using the model given in Table 2.1. (b) Complex species percentage distribution curves of homopiperazine-copper system (1:2 ratios) as a function of pH.

(a) (b)

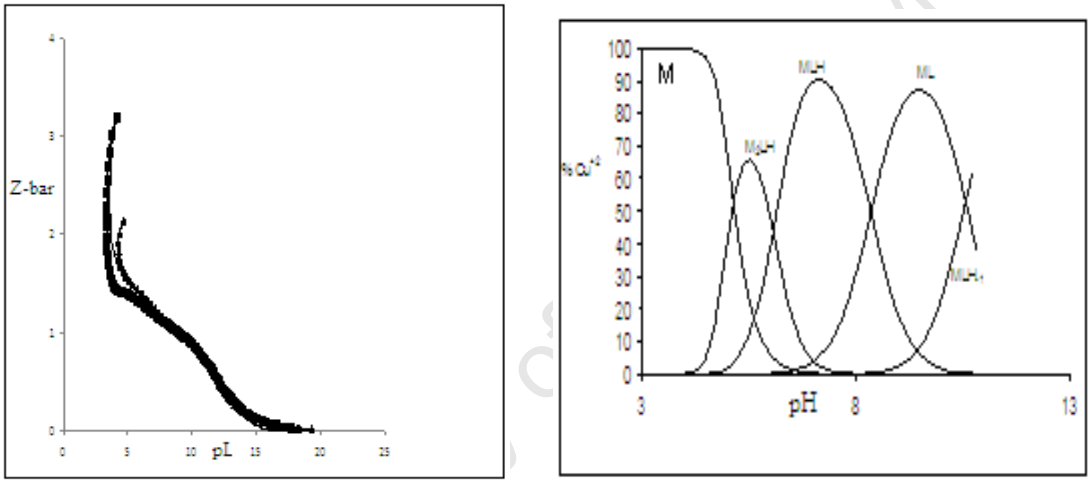

Figure 2.6 (a) shows the Z_M-bar function for Cu(II)-PCU.homo system plotted against pL. After the start of the titration (i.e. pL>15), the formation function rises and levels off at Z_M-bar value of 1.6, thus indicating that the mononuclear ML species is not the only dominant species formed in solution in the physiological pH range. The different symbols used, represents different metal to ligand ratios. At low pL values (i.e. pL< 5) the curves fan back, thus indicating the formation of hydroxo or mixed-hydroxo complex species in solution. Excellent agreement between the theoretical and experimental complex formation curves at different metal to ligand ratios supports the potentiometric model chosen in data analysis. From Table 2.2, the reported standard deviation of the log β_{pqr} values obtained from potentiometry are reasonably low, but the R_f^H is

equal to its limit and this indicates that the model chosen to investigate this system cannot be improved any further.

Table 2.: $\log\beta_{pqr}$ of PCU.homopiperazine-Cu(II) system determined at 25°C in 0.15 mol.dm^{-3} (Cl^- Na^+). S. dev denotes standard deviation in $\log\beta_{pqr}$; R_f^H is the Hamilton R-factor and R_{lim}^H its limit. The general formula of a complex is $M_pL_qH_r$ denoted by the stoichiometric coefficient pqr.

LIGANDS	p q r	Log β	S.dev	$R._{lim}^H$	$R._f^H$
PCU.homo-Cu^{+2}	2 1 1	21.22	0.03	0.02	0.02
	1 1 1	17.60	0.03		
	1 1 0	9.25	0.02		
	1 1 -1	-1.39	0.03		

2.7.2.3.2 Structure discussion – Complexation

An interesting feature about the speciation graph (Figure 2.6(b)) is that at the start of the titration M_2LH is the dominant species at low pH values. The ligand system in this study is based on two diene moieties linked to a rigid cage and these contain ethylene and propyle linkages. Upon complexation the amines should lose a proton. During this period the solution will be buffered and furthermore the rigid cage on PCU.homo should limit the number of conformations that the free ligand will have. This is expected to drive the equilibrium towards complex formation. However in order to explain the observed complex stability, a series of structures have been proposed for the different species (Figure 2.7), based on the equilibria in Table 2.2.

Figure 2.7: Schematic representation of proposed structures of various Cu(II)-PCU.homo species. Water molecules coordinated to the Cu(II) and cage moiety are omitted for clarity.

M_2LH

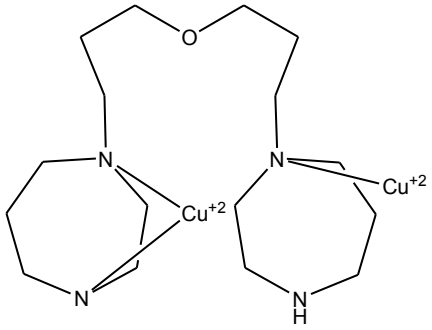

(a)

MLH

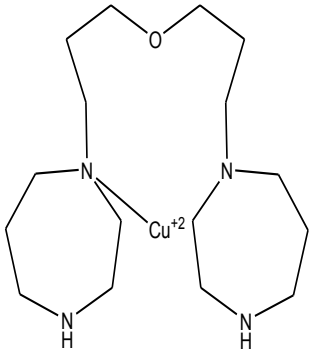

(b)

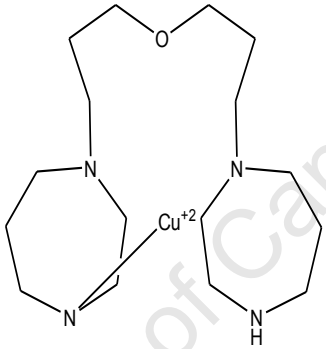

(c)

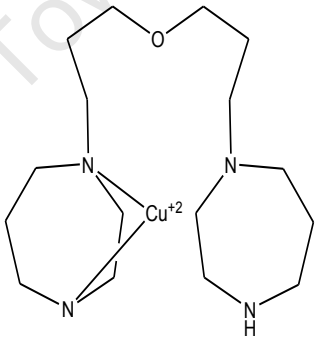

(d)

ML

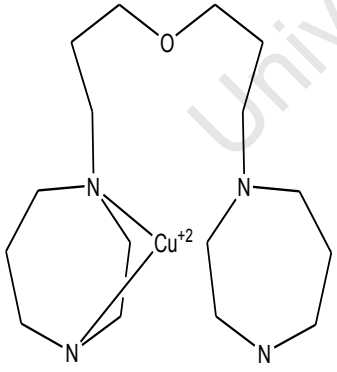

(e)

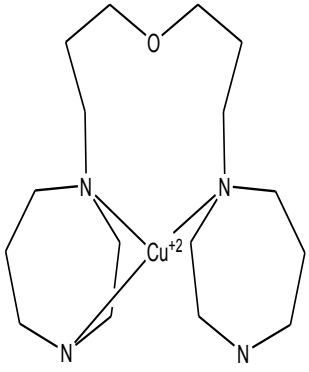

(f)

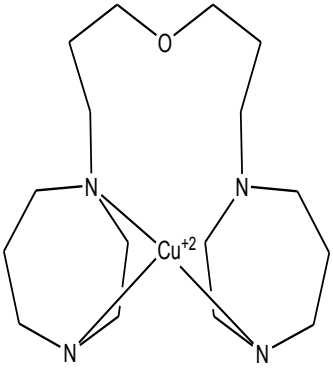

(g)

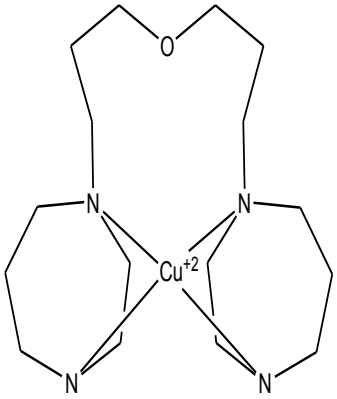

(h)

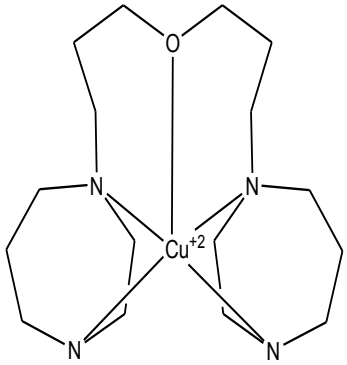

(i)

MLH_{-1}

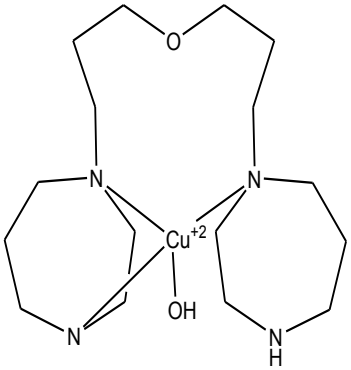

(j)

The proposed structures for the MLH species of the metal ion-ligand complex in the present study are given in Figure 2.7(b-d). In 2.7 (b and c) the metal ion is coordinated to only one of the 4 nitrogens, while one of the nitrogens on the other homopiperazine is still protonated. However this structure is unlikely because, if we consider the equilibria: $M + LH \rightleftharpoons MLH$, with an equilibrium constant of 7.3 (i.e. $\log\beta_{111} - \log\beta_{011}$). This value is too high for a monodentate coordination of the metal ion. In fact this value is close to the equilibrium constant of ML of homopiperazine ($\log\beta_{110}$ =7.6, see Table 1.1). Because of the chelate effect it is also unlikely that only one of the nitrogens of the homopiperazine would coordinate to the metal ion [15-17]. Similarly, if we consider M_2LH to be formed by coordination of a second Cu(II) ion to the MLH species, a stepwise log equilibrium constant of 3.62 can be calculated from $\log\beta_{211} - \log\beta_{111}$. This is very close to $\log\beta_{110}$ obtained for Cu(II)/methylamine which is 4.11 [10]. Therefore it was conclude that the second Cu(II) ion must be monodentately coordinated to the second homopiperazine moiety on PCU.homo. Furthermore the equilibrium constant for M_2LH is 2 orders of magnitude less than the pK_4 (5.44) of the free ligand. This must be due to the presence of the metal ion, either through columbic repulsion or through a different nitrogen being protonated. Therefore (a) was chosen as the most likely representation of the M_2LH species. Assuming that structure (d) is correct for the MLH species, then formation of ML species occurs with a pK_a of 8.35 (i.e. $\log\beta_{111} - \log\beta_{110}$). This deprotonation could happen on its own (structure e) or with simultaneous coordination of the metal ion.

Since the equilibrium constant of the ML species is close to the pK_a 9.11 of the terminal amine, therefore it will be safe to assume that the proton lost is from this amine upon coordination to the copper (II). The K_a of ML (PCU.homo) is 0.75 log units higher than the $\log\beta_{110}$ (7.6) of the ML for HP. This suggests that the coordination geometry of the ML species involves more than two amines coordinated to the central metal ion. Comparing the structures (f) and (g), both structures will be stabilized by the coordination of the third amine thus forming a [5, 13] and [5, 10] membered chelate rings for (f) and (g) respectively.

Structure (h) was eliminated based on the difference in stability constants between the ML species (β_{110} =9.25) of PCU.homo and the ML_2 species of HP (β_{120} = 12.6) which is 3.35 log units, therefore it is unlikely that the complex structure of ML would involve all 4 amine donor groups being coordinated to the metal ion.

Similarly (i) was also eliminated because the value of the equilibrium constant (K_a = 8.35) for the ML of PCU.homo lies between the equilibrium constant of the ML (log β_{110} = 7.6) and ML_2 (log β_{120} = 12.6) for HP. Therefore the coordination geometry of the ML species does not involve 4 amines coordinated to the metal ion. Furthermore the binding of oxygen in the axial position will further destabilize the complex, putting more strain on the complex.

The overall order of the stability constants for ML species of the two related ligand system PCU.EN and PCU.homo is revealed to be PCU.EN (4N donor) [23] > PCU.homo. The low stability constants observed for the ML species for PCU.homo- copper (II) system can be attributed to the steric effect on the PCU.homo caused by the cyclic nature on the amine nitrogen in homopiperazine moiety.

Deprotonation of ML with a pKa ($\log\beta_{110} - \log\beta_{11\text{-}1}$) of 10.64 results in the formation of the MLH_{-1} species. This value is similar to the pK_1 of $[Cu(II)(H_2O)_6]^{+2}$ (10.65) assigned to the deprotonation of the axial water molecule reported by Jackson *et al.* [7]. Therefore the structure of MLH_{-1} was proposed to be (j).

2.7.2.4 Zn(II)-[PCU.homopiperazine] system

The study of the solution chemistry of Zn(II)-PCU.homo system was complicated by the formation of a precipitate at pH 7. Furthermore no metal ligand interaction was detected with different metal to ligand ratios used thus making the determination of stability constants of the various species that might form in solution for this system impossible using the glass electrode. It is worth mentioning that the same observation was noticed with the Zn(II)-HP system [14], this was concluded as being caused by the cyclic nature of the ligand 'homopiperazine' which is believed to find it difficult to form a tetrahedral geometry around zinc, and this leads to a weaker complex being formed.

Reference:

1. K. Murray and P.M. May. Univ. Of Wales Institute of Science and Technology (1984).
2. F. R. Hartley, C.Burgess and R.Alcock, Solution Equilibria(1980), Ellis Horwood, Chicherster
3. P.M. May and K. Murray and D.R.Williams, Talanta, 32, (1974) p. 53
4. H. Rossoti. The Study of Ionic Equibria, (1978), Longmans, New York
5. P.W. Linder, R.G. Torrington and D.R.Williams, Analysis Using Glass Electrodes, 1984, Open University
6. J.C Rossotti and H. Rossoti, The determination of stability constants in solution, (1961), McGraw Hill, New York
7. E.T Nomkoko., G.E Jackson., B.S. Nakani., S.A Bourne. J. Chem. Soc., Dalton Trans, (2004), p. 1789
8. T. A Kaden and A. D. Zuberbuhler, Helv.chim Acta, 57 (1974) p. 286
9. M. Kodama and E. Kimura, J.Chem. Soc. Dalton, (1980), p. 327
10. R.D.Hancock. J. Chem. Soc Dalton, (1980) p. 416
11. R. Machida, E. Kimura, and M. Kodama, Inorg. Chem, 22 (1983) p. 2005
12. C.F. Baes Jr. and R.E. Mesmer. The Hydrolysis of Cations, p. 268, 1976, Wiley Interscience, New York,
13. B.S Furniss., A.J Hannaford., P.W.G Smith., A.R Tatchell., *Vogel's Textbook of Practical Organic Chemistry*, 5th ed, 1989, Longman Scientific and Technical, England
14. G. Gran. *Analyst*, 77 (1952) p. 661-671
15. S. Odisitse., *MSc Thesis*, 2003, University of Cape Town, South Africa
16. I. Karin, G. Gerrit Herman, C. Fabretti, W. Lippens and M.A. Goeminne, J.Chem Soc., Dalton Trans., (1996), p 1753-1760
17. D.L Leussing, Inorg Chem., 2,(1963), p 77
18. D. E. Golgberg and C. W. J Fernelius. Phys. Chem. 8 (1959) p.1246-1249

19. H. Gampp, D. Haspra, M. Macder, and A.D. Zuberbuhler, Inorg. Chem. 23 (1984) p. 372

20. A. Bianchi, E. Garcia-Espan, M. Miehelai, J. Antonio Ramirez. Coordination Chemistry Reviews. 188 (1999) p.97-156

21. K.I. Dhont, G.G Herman, A.C Fabretti, W Lippens and A.M Goeminne. Protonation and metal ion complexation in aqueous solution by pyridine containing hexaaza macrocycles. J. Chem. Soc., Dalton Trans.,(1996) p.1753-1760

22. S. Odisitse, G. E. Jackson, T. Govender, H. Kruger and A. Singh. Chemical speciation of copper (II) diaminediamide derivative of pentacycloundecane-a potential anti-inflammation agent. Dalton Trans., (2007) p.1140-1149

23. K. Mokalane Hons Thesis, 2008, University of Cape Town, South Africa

24. A.E. Martell, R. M Smith and R.J Motekaitis, National Institute of science and Technology (NIST) Critical Stability Constants of Metal Complexes Database , NIST Standard Reference Database 46, (1993) Giathersburg, MD, VCH Publishers Inc., New York.

CHARPTER 3:

NMR SPECTROSCOPY STUDIES

3.1 NUCLEAR MAGNETIC RESONANCE

3.1 Introduction

In order to determine explicitly the structures of various species formed in solution a number of spectroscopic techniques can be utilized; these include NMR, Infrared, Raman or/and UV/VIS spectroscopy [1]. However the use of nuclear magnetic resonance (NMR) as an important tool in structure and reaction mechanism determinations in aqua has grown significantly over the past decade and recently its use has been extended to in full body imaging (MRI) [1-2]. Similarly the use of NMR to determine acid-base equilibrium protonation constants for substances of biological importance, particularly amine groups, has increased considerably in the past 3 decades. NMR spectroscopy has an advantage over potentiometric titration, in that NMR can be used to estimate protonation constants of organic ligands directly from biological mediums of physiological importance such as blood plasma [2] and urine which contain other acid and bases in solution by following the chemical shift of nuclei of interest as a function of pH or pD. However in this study NMR was used to determine the sequence of protonation of the four amine groups on PCU.homopiperazine in water as a function of pH and to elucidate the complex structure it forms when coordinated to Cu(II) ion. This is done by observing the change in chemical shift of protons on neighbouring (i.e. alpha position relative to amine group) carbons as a result of a proton being attached to an amine group [3]. Similarly the presence and or coordination of the paramagnetic metal ion (i.e. Cu(II)) is expected to broaden and change the chemical shift arising from α protons [4, 5], thus giving a clue about the coordination mechanism between the ligand and metal ion and the structure of the complex formed in solution [5]. The change in chemical shifts of ^{1}H spectra were analysed by plotting the $\Delta\delta$ as a function of pH (see Figure 3.2). The inflection point in the curve of change in chemical shift as a function of pH can be used to obtain estimates of the equilibrium/protonation constants for the system.

3.2 Experimental

1 ml of PCU.homopiperazine solution (7.6mM) in D_2O was freeze dried with a vacuum drier to remove excess water from the ligand. The ^1H NMR spectra were recorded on a Varian Unity Plus 400 MHz instrument. The pH of the solution was measured using a micro-pH 2000 meter. The pH meter was then calibrated in terms of deuterium ion activity as follows [4].

pD= pH + 0.4

For protonation and complexation titrations, no attempt was made to keep the ionic strength of the solution constant.

For the protonation scan, 7.6mM stock solution of PCU.homopiperazine was prepared in a 1ml glass vial, by dissolving the solid ligand in 1 ml D_2O and a few drops of tertiary butyl alcohol were added to serve as a reference signal. The pD of the solution was adjusted by adding concentrated NaOD and DCl solutions.

The solution was then transferred into a 5 mm NMR tube for measurement of the ^1H NMR spectrum. After recording of the spectrum the solution was transferred back into the vial (with at least 95% recovery) and pD measured again. Agreement of the pD values before and after measurement of the nmr spectrum was within 0.02 pD units. A known volume of NaOD or DCl was then added and the sequence – (measure pD, →record spectra, → measure pD, →add base or acid) – repeated until pH 11 was reached.

To obtain the ^1H resonance spectra of the copper (II) complex, the freeze dried ligand was dissolved in 1ml of D_2O to the same concentration as in the protonation experiments (7.6mM) and adjusted to approximately pH 5 using NaOD. Tertiary butyl alcohol was used as an internal reference. For each scan a 20 µl aliquot of copper solution was added until a two- fold excess of copper had been added.

3.3 Results and Discussion

Figure 3.1(a) shows the ^{1}H NMR spectrum for protonation of PCU.homopiperazine in D_2O as a function of pH. From Figure 3.1 (a) throughout the pH range 1.32 to 9.89 the ^{1}H signals labelled a, b, c, d, e, and f all shift significantly up-field, while the ^{1}H resonance signals labelled m, i, j and k remained constant. As a result the latter signals were assigned to the the adamantane cage.(see Figure 3.1(b)). At high pH, analysis of the spectra was complicated by the fact that the PCU.homopiperazine has chemically equivalent CH_2 and CH groups, resulting in signal overlap. Therefore a $^{1}H/^{1}H$ COSY spectrum at pH 8 was used to unequivalently identify/assign the proton signals at 2.8 ppm and 3.2 ppm. The 2D spectrum was also used to follow the chemical shift of the protons α to the terminal amines (i.e. a and\or c). In Figure 3.1(c), the multiplet signal at 2.1 ppm labelled peak d is correlated to two resonances at 2.8 ppm and 3.2 ppm, and hence these were assigned to protons e and c respectively. A CH_2 peak labelled 'a' on the 2D spectrum appearing as a doublet at 3.2 ppm has only one cross peak at 2.9 ppm and this resonances is assigned to proton b. Similarly a second CH_2 peak labelled f at 3.3 ppm has one cross peak at 2.2 ppm, which can then be assigned to proton g. At the start of the titration, at low pH (i.e. 'between' 1.32 - 4.65) there is no observed change in the chemical shifts. This indicates that no proton is removed from the ligand and the ligand exists as a fully protonated LH_4 species.

Figure 3.1(a): ^{1}H NMR spectra of PCU.homopiperazine as a function of pH. Chemical shifts are given relative to tertiary butyl alcohol as an internal standard. (b) Structural formula of PCU.homopiperazine showing atom labelling. (c) $^{1}H\backslash^{1}H$ correlated spectrum (COSY) of PCU.homopiperazine at pH = 8. Chemical shifts are given relative to tertiary butyl alcohol as an internal standard. (d) $^{1}H\backslash^{13}C$ Heteronuclear Correlation spectrum (HSQC) of 7.9952 mM PCU.Homopiperazine solution in D_2O at pH = 8.

(a)

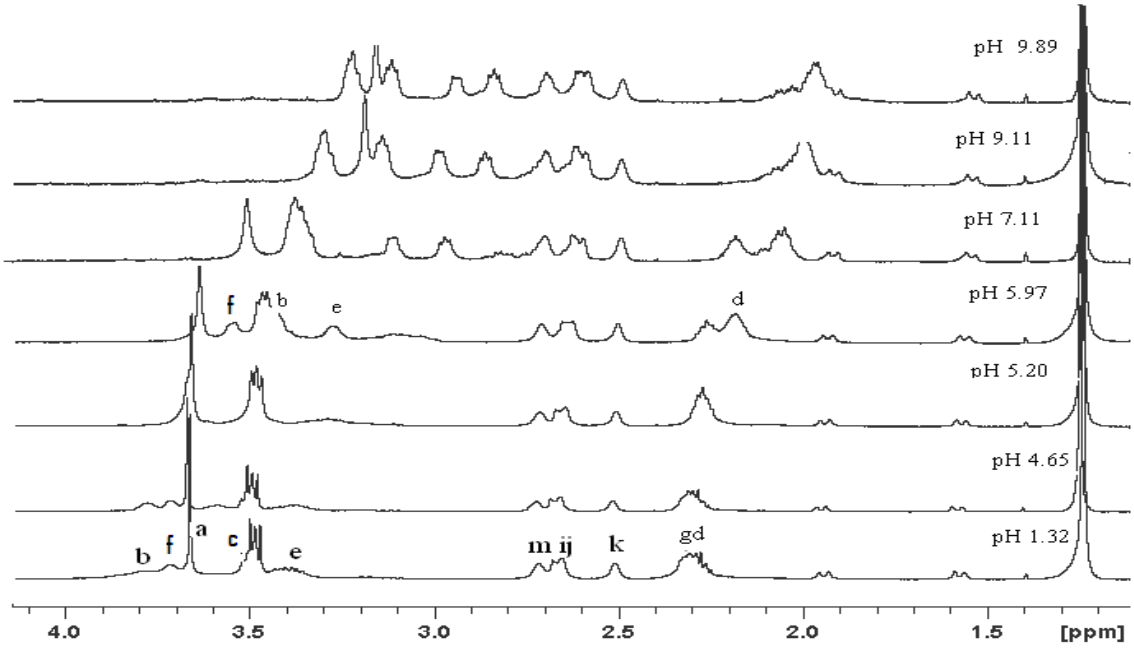

b

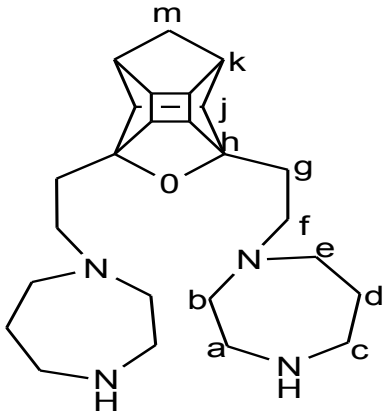

c

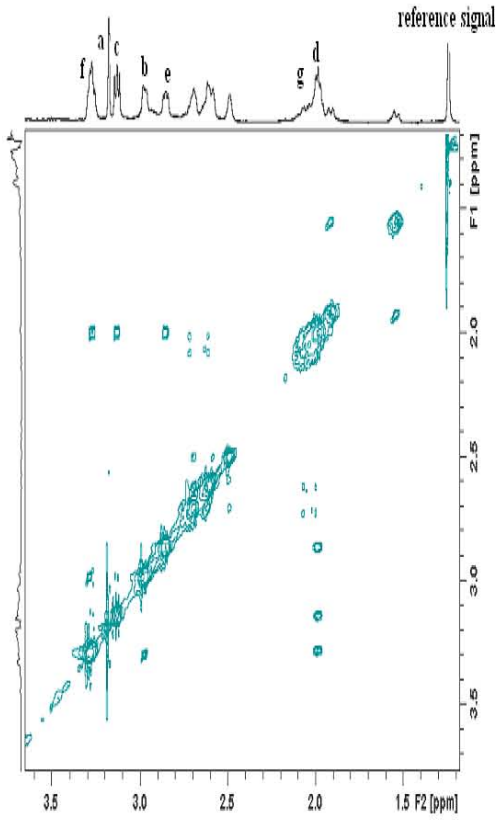
reference signal
a
c
f
b
e
g
d
F1 [ppm]
2.0
2.5
3.0
3.5
3.5
3.0
2.5
2.0
1.5 F2 [ppm]

d

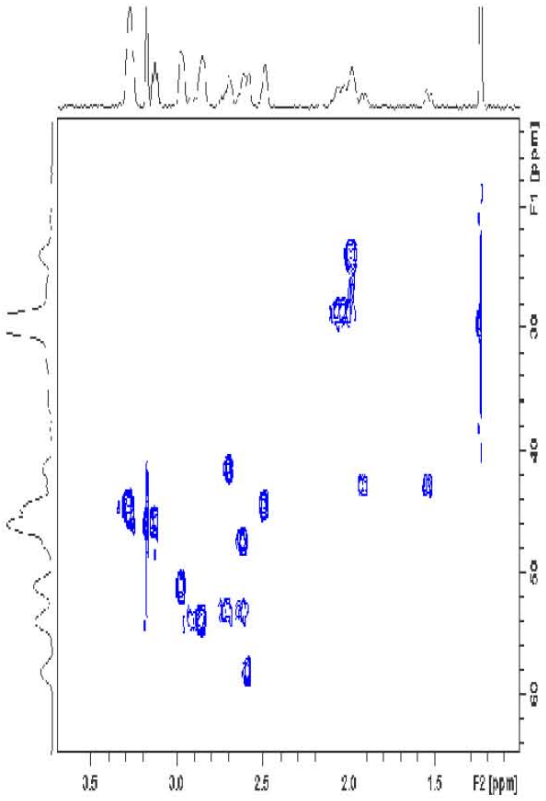
F1 [ppm]
30
40
50
60
3.5
3.0
2.5
2.0
1.5
F2 [ppm]

Figure 3.2 Plot of change in ^{1}H NMR chemical shift of PCU.homopiperazine as a function of pH.

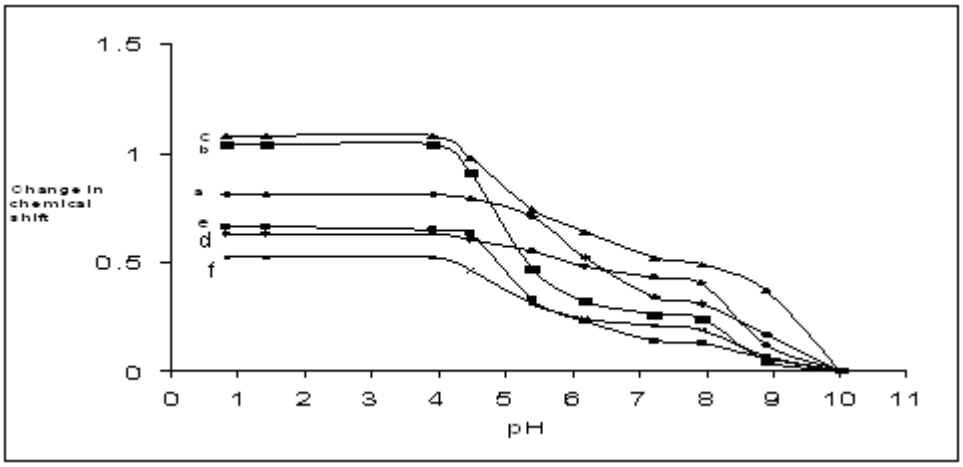

Figure 3.2 shows the plots of change in proton chemical shifts as a function of pH, where a, c and b, e, f refer to the chemical shift of the protons attached to carbons next to the secondary and tertiary amine groups respectively. d refers to the proton attached to the carbon in the beta position in the homopiperazine (i.e. heterocyclic moiety on the ligand) see Figure 3.1(b). From Figure 3.2, between pH 2-6 the ^{1}H signals labelled b, e, and f are shifted significantly up-field , while the ^{1}H signals labelled a, c and d remain fairly constant. This suggests that the former signals are close to the site of protonation which must be the tertiary amines. From this change in chemical shift plot, the micro-protonation constant of the tertiary amine is estimated to be 5.2, which is close to pK_{a4} obtained from potentiometry. However the chemical shift for the signals a and b changes considerably in the pH range 7-10. This is mainly attributed to the fact that the two protons a and b are closer to the amine groups where protonation takes place, thus indicating the protonation of the secondary amines. Again approximate values for p$K_{1,2}$ are estimated to be 9 and 10. This is in good agreement with the values obtained from potentiometric studies. The proton assignments are confirmed by the HSQC spectrum (Figure 3.1(d))

Figure 3.3 Protonation scheme for PCU.homopiperazine based on NMR experiments, the cage structure/moety has been omitted from the structures for clarity.

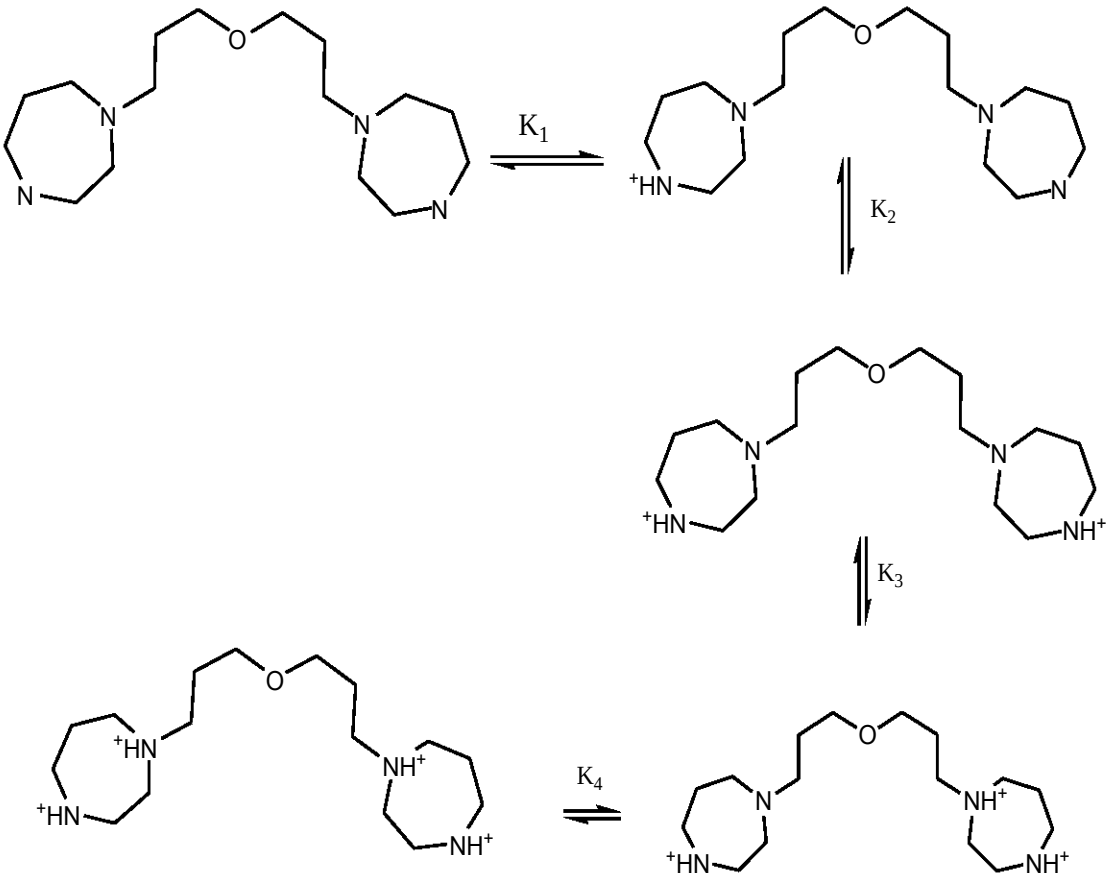

The ^{1}H spectra of the Cu(II)-PCU.homo system as a function of Cu(II) concentration are shown in Figure 3.4 (a). Copper (II) is paramagnetic, so it is expected to cause the proton peaks near the metal ion to broaden and shift down field. In Figure 3.4(b), the signals of a, c, and d broaden and shift downfield as the concentration of copper is increased. The rest of the signals remain almost unchanged. This result suggests that complexation has taken place with only the secondary amines (either one or both) coordinated to the central metal ion. From potentiometry, at this pH = 7.23, the MLH species is the dominant species. Furthermore, in Figure 3.4(a) more amine groups are close to the copper (II) ion centre. This is indicated by signals arising from protons (a, b, c, d, e, and f) which are attached to carbons closer to the amine groups broadening considerably and with signals a, c, and f almost disappearing as the concentration of the metal is increased further. In this region of pH = 8.1, the ML species predominates. However from close inspection of the ^{1}H spectrum, signals b and e do not broaden and shift to the same extend as the other signals, thus suggesting that the coordination geometry in ML species involves two secondary amines (i.e. the terminal amines) and one tertiary amine being coordinated to copper (II) with the other tertiary amine uncoordinated. This is consistent with the result from potentiometry. However the decision of how many amine groups are actually attached to the central metal ion is made more difficult by the fact that over the entire concentration range only single resonances for non-equivalent protons are observed, indicating that the ligand is in rapid exchange between isomers. This problem is solved in the next section.

Figure 3.4 ^{1}H NMR spectra for complexation of copper (II) with PCU.homopiperazine as a function of copper (II) concentration.

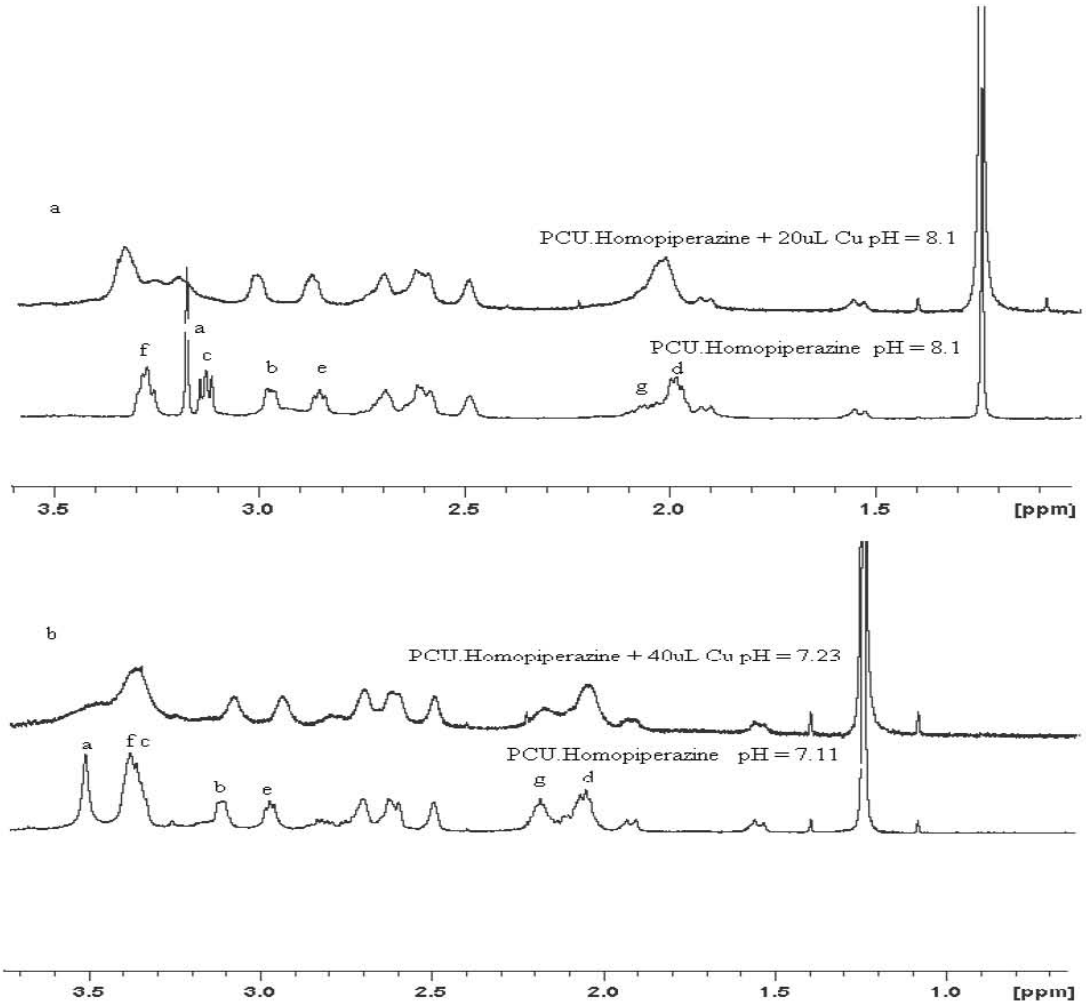

Reference:

1. T. E. Nomkoko, G. E. Jackson, B. S. Nakani and R. Hunter. Solution chemistry of 1,15-bis(NN-dimethyl)-5,11-dioxo-8-(N-benzyl)-1,4,8,12,15-pentaazadecane with metal ions of biological interest-Insights toward active metal ion containing therapeutic and diagnostic agents., Dalton Trans. 40 (2006) p.29-4038.
2. J.W. N.m.r and Chemistry: Introduction to the Fourier transform-multinuclear era. Chapman and Hall (1983).
3. E. T Nomkoko, G. E. Jackson., B. S. Nakani, S. A. Bourne. J. Chem. Soc. Dalton Trans, (2004) p. 1789
4. R.D.Hancock, J.Chem. Soc Dalton Trans, (1980) p. 416
5. T. Axenrod and G.A. Webb., Nuclear Magnetic Resonance Spectroscopy of nuclei other than protons (1973). Chapters 1, 2 and 3.
6. R.J. Abraham., Analysis of High Resolution NMR Spectra. Academic Press (1966). New York Chapters 1-3.

CHAPTER 4:

UV/VISIBLE SPECTROPHOTOMETRY AND MOLECULAR MECHANICS CALCULATIONS (MM)

4.1 UV-VISIBLE SPECTROSCOPY

4.1.1 Introduction

An obvious difference between certain compounds is their colour. Examples include quinone which is yellow; chlorophyll that is green and copper (II) sulphate which is blue [1]. In this respect the human eye is functioning as a spectrometer analyzing the light reflected from the surface of a solid or passing through a liquid. Electromagnetic radiation such as visible light is commonly treated as a wave phenomenon, characterized by a wavelength or frequency [2]. Visible wavelengths cover a range from approximately 400 to 800 nm [1, 2]. Spectrophotometry uses the visible region of the electromagnetic spectrum to give an idea of the electronic microstructure of metal systems, by quantifying the amount of light absorbed by the system [2]. This is because the amount of light a transition metal species will absorb directly depends on type of metal ion, its oxidation state, electronic configuration of the metal and the type of ligands surrounding it [2, 3]. As a result spectrophotometry is used extensively in literature for the study of solution chemistry of transition metal ion complexes [3, 4]. This is due to the various colours that are observed for transition metal complexes, which are caused by electronic transition between energy levels, whose spacing corresponds to the wavelengths available in visible light [2, 3-5].

4.1.2 Electronic Spectra of Metal Complex

When a molecule absorbs light of a suitable frequency, it assumes an exited state in which some of its electrons occupy higher energy levels, which only differ from the parent molecule by the distribution of its electrons and thus contains new chemical properties such as a different structure and energy state [3-5]. These transitions are frequently referred to as d-d transitions because they involve molecular orbital that are characteristic of transition metals. However the intensity of the absorption bands is governed by a series of selection rules [4]. Transitions that are Laporte forbidden are those between orbitals of the same symmetry gerade to gerade (g-g) or

ungerade to ungerade (u-u) respectively, because there is no change of parity [3-4]. Those transitions that are allowed according to Laporte include transitions between gerade to ungerade or vice versa. This therefore means that all d-d transitions are forbidden. However transitions can occur if the symmetry of the molecule is removed. The bonds in transition metal complexes are not rigid but undergo vibration that temporarily changes the symmetry of the molecule [5]. This distortion from a perfect octahedral geometry increases the transition probability and hence the intensity of the transition [5]. In a tetrahedral ligand field environment there is no centre of symmetry and therefore the orbital may acquire some p-orbital character, thus allowing the forbidden d-d transition to be partially allowed [5].

4.1.3 Electronic Spectra of Copper Complexes

The chromophoric nature of the copper (II) ion is due to its low-lying d-orbitals [4, 6]. Many copper complexes absorb light in the visible region of (400-800 nm), and the characteristic d-d absorption band changes its absorbance maxima according to ligands around the metal ion centre [3-7]. The aqueous chemistry of copper is largely focused on copper (II) complexes because they are more stable than copper (I) complexes in aqueous solutions [4] and of course Cu(I), being d^{10} has no d-d transitions. Tetragonal distorted copper (II) shows a single broad poorly resolved absorption band in the visible region [4]. This belongs to three absorption bands, corresponding to the following electronic transitions:

$^2A_{1g}$ - $^2B_{1g}$

$^2B_{2g}$ - $^2B_{1g}$

^2E_g - $^2B_{1g}$

$CuSO_4.5H_2O$ and many copper (II) salts are blue, and this is because they absorb light in the regions between 540-800 nm [2-5]. The absorption spectrum of a copper (II) complex involving amine groups as a ligands, have been shown to be pH dependent [7]. As the pH increases the ligand becomes deprotonated and coordinates to the metal ion displacing coordinated water molecules. This causes a blue shift in the absorption maximum of the metal ion (i.e. shorter

wavelength) [5-7]. This is extensively reported for copper (II) complexes with 6 waters as ligands, which normally shows an absorption maximum at 800 nm [4-6]. If the four water molecules in the equatorial position on metal ion were to be substituted with four ammonia ligands, this would cause the metal to shift its absorption maximum to around 600 nm [3-6]. This shift can be explained, as being caused by the strong ligand field splitting of the nitrogen atoms. However it has been recently reported that coordination on the axial position causes a red shift in the absorption maximum of the band [5-6]. This indicates that when the electronic nature of the central ion is known, it can therefore be used to suggest the nature or number of the ligands surrounding the metal ion [7] and thus give an approximation of the structure that is formed in solution [7-8].

Most copper (II) complexes that have been studied have been found to have distorted octahedral structures, and this is as a consequence of the unfilled d-orbital configuration of d^9 on the metal ion [7]. This d^9 (i.e. e_g^3 and t_{2g}^6) configuration results in the uneven filling of the e_g orbital which results in a well known phenomenon called Jahn-Teller distortion. Jahn-Teller distortion causes the two ligands placed at axial positions and trans to each other to move away from the central metal ion until such a state where their inter nuclear distance is greater than that of the four remaining ligands place at equatorial positions [4]. At this stage the complex is said to have tetragonally distorted geometry [3-5]. Looking at the electronic distribution of copper (II) d^9, one would expect copper (II) to have only one absorbance peak, but because of the Jahn-Teller distortion the degeneracy of the electronic energy levels is lifted. This results in a shoulder on the expected absorbance peak [6]. Cu(II) ions have been found to form complexes with polydentate ligands with nitrogen as a coordinating atom and the resultant structures were found to be dependent on both the number of the donor atoms and the steric requirement of the ligand [7].

4.1.4 Data Analysis

Since the amount of light absorbed by a medium is directly dependent on the number of absorbing species within that medium, (A) absorbance can be used to estimate the concentration of the participating species in solution [7, 8].

This is because the amount of light absorbed by a system can be related to the concentration of its absorbing species using the Beer-Lambert Law, given by;

$$A = \log I_0 / I = \varepsilon c l \qquad (4.1.1)$$

Where: c is the species concentration in $mol.dm^{-3}$,

ε is the molar absorptivity and

l is the optical path length.

I_0 is the intensity of incident ray

I is the intensity of the emergent ray

For a solution of known species concentration and a given path length, the absorbance is dependent on the specific molar absorptivity coefficient of the species of interest [2, 3, 8-10]. For electronic absorption spectra of solutions containing more than one absorbing species at a particular wavelength the Beer-Lambert law can be expanded to give a linear combination of terms for each individual species [7-10], Equation 4.1.1

$$A^{\lambda} = l (\varepsilon_1^{\lambda} c_1 + \varepsilon_2^{\lambda} c_2 + \ldots + \varepsilon_i^{\lambda} c_i) = l \sum \varepsilon_i^{\lambda} c_i \qquad (4.1.2)$$

Where: A^{λ} = Absorption at wavelength (λ nm)

ε_i^{λ} = molar adsorption coeffient at wavelength λ of the i^{th} species ($dm^3 mol^{-1} cm^{-1}$)

c_i = concentration of the i^{th} the species ($mol.dm^{-3}$)

l = cell path length (cm).

Therefore if a certain species has a value of ε^{λ} equal to zero, then it does not absorb in the chosen spectral region and it does not have any effect on the A_{obs}^{λ} [7-9].

Billo has developed a simple empirical method which can be used to calculate the total electronic transition energy contribution from donor atoms in the coordination sphere of the metal ion [9]. This is given by the following:

$V_{calc} = \sum V_i$

Where: V_i is the energy contribution of each donor atom, see Table 3.1.

Table 3.1: Energy contributions to the coordination sphere of some donor atoms as proposed by Billo for a system involving Cu(II).

Donor atoms/groups	Energy contribution (cm^{-1})
Amide	$4.85 \pm 0.04 \times 10^3$
Amine	$4.53 \pm 0.07 \times 10^3$
Carbonyl oxygen, H_2O, OH^-	$3.01 \pm 0.03 \times 10^3$
Carboxylate oxygen atom	$3.42 \pm 0.10 \times 10^3$
Oxime nitrogen	3.38×10^3

Furthermore the nature of electronic transitions that are brought about by a chelating ligand can be inferred from general observation of the effect of monodentate ligands on the ligand field parameter [10]. Table 3.2 shows a guideline that is normally used for the estimation of the effect of the ligand field imposed by nitrogen based donor ligands [11].

Table 3.2 the absorption maxima of the Cu(II) ammine complexes of the general formula $[Cu(II)(NH_3)_n(H_20)_{6-n}]^{+2}$

N	Absorption maximum (nm)
0	790
1	745
2	680
3	645
4	590

4.1.5 Experimental

Spectrophotometric titrations were performed for Cu(II) complexation with PCU.homopiperazine. These solutions were prepared in the same way as the solutions used to determine formation constant using potentiometry. An aqueous solution containing 1:2 metals to ligand ratio was prepared in a quartz corvette of 1 cm length and the complex spectra were measured over the pH range 4-10. Small amounts of 0.0995 M NaOH were used to adjust the pH of the solution. The pH of the solution was monitored using a micro-pH 2000 meter. Before any pH measurement could be done, the micro-pH 2000 was calibrated with commercial standards of known pH values (i.e. 4.00, 6.78 and 9) at 25ºC. The calibration procedure was repeated every time after the solution's pH change by 2 units. The solution was kept at a temperature of 25˚C and the titration was allowed to proceed under a nitrogen gas flow. Spectrophotometric measurements were recorded using a Hewllet Packard 8452 A Diode Array Spectrophotometer, in the wavelength range of 300-800 nm and deionised water was used a reference.

4.1.6 Results and discussion

The PCU.homopiperazine ligand system is an ON_4 type ligand capable of donating four nitrogen atoms (amine groups). The ligand also has ether oxygen capable of coordinating to a metal ion. During the pH titration, the solution of PCU.homo-Cu(II) showed a colour change from blue to violet as the pH was increased and this was concluded as being the effect of change in speciation in the solution as a result of coordination of different aza-donor atoms to Cu(II) ion [8]. This further meant a change in the absorption maxima of the solution's dominant species [8]. In order to gain some insight into the coordination geometries of the different species in solution, their individual spectra were calculated from the total absorbance. The deconvulation of the UV/Vis data [9] was performed using the UV-SPEC program. Absorption spectra obtained in the pH range 4.4-10.6 are shown in Figure 4.1(a) and the deconvoluted spectra in 4.1(b) respectively.

Figure 4.1(a) Absorption Electronic spectra of Cu(II) and PCU.homo in solution in the wavelength range 300-800 as a function of pH. (b) Deconvoluted electronic spectra of solution of Cu(II) - PCU.Homo system as a function of wavelength.

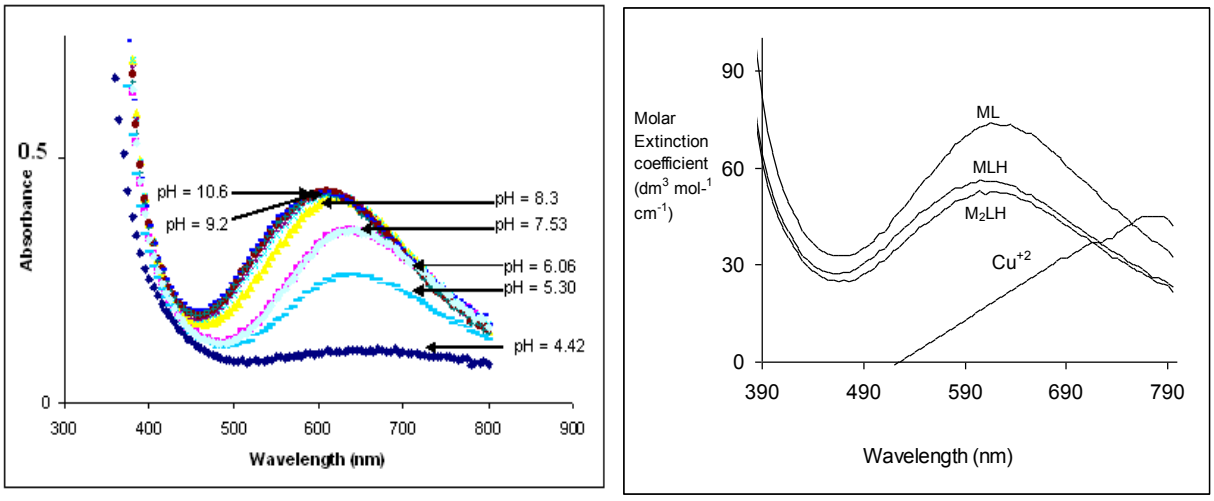

Figure 4.1(a) shows the electronic spectra of Cu(II) and PCU.homo in solution in the wavelength range 300-800nm as a function of pH and Figure 4.1(b) shows a graph of molar absorption coefficient, ε, as a function of wavelength for Cu(II) complex species with PCU.homopiperazine.

The broad absorption bands observed in Figure 4.1(b) corresponds to the three overlapping, spin allowed, Larporte forbidden transitions, $^2A_{1g} \leftarrow {}^2B_{1g}$, $^2B_{2g} \leftarrow {}^2B_{1g}$, and $^2E_g \leftarrow {}^2B_{1g}$, characteristic of d^9 tetragonally distorted Cu(II) complexes [14]. In the deconvolution, each wavelength is treated independently so the smoothness of the resultant deconvoluted spectra lends confidence to the spectra obtained and the model used to explain the PCU.homo-Cu(II) system. As can be seen from Figure 4.1(a), at pH 4.5, there is no complexation taking place and this is indicated by a band with an absorption maximum of 790 nm, which corresponds to the absorbance maximum of the free hydrated copper species (i.e. [Cu(II) $(H_2O)_6]^{+2}$) [8, 9, 10]. As the pH of solution is increased the absorbance of the solution increases and shifts to shorter wavelength as the pH is increased between pH's 4.8 and 6, this is caused by coordination of the some amine groups to the Cu(II) ion. The MLH species, with maximum wavelength of 650 nm and a molar extinction coefficient (ε) 55.63 $dm^3.mol^{-1}.cm^{-1}$, is the dominant species in the pH range 4.8-6.0 (see potentiometric results Section 2).

A further increase in the pH from 6 to 10 caused the absorption band to shift to a shorter wavelength (i.e. 600 nm) and there is also an increase in the intensity of the absorption band. This extra intensity of the absorption band is caused by increase distortion of the metal coordination geometry resulting from the binding of more nitrogen donor groups to the metal ion centre (i.e. Cu(II) ion). From potentiometry speciation (Section 2, see Figure 2.3(b)), ML is the dominant species in this pH range. The ML species has a molar extinction coefficient of (ε) = 71.24 $dm^3.mol^{-1}.cm^{-1}$. At pH's > 10, no further change in the absorbance band could be observed indicating the ending of complexation or no change in the ligand field of the metal ion. From the speciation results, the MLH_{-1} species should predominate in this region. Hence it was concluded that λ_{max} and ε are the same for both ML and MLH_{-1} species. The absence of an isosbestic point in the absorption band in this pH range, further confirms that the structure of different complex (i.e. MLH, ML and MLH_{-1} species) being formed in solution as a function of pH are not different from one another or it can be concluded that the system does not undergo a considerable

conformational changes when moving from one species to the next. According to Billo, water has the same crystal field effect as OH^-.

4.1.7 Discussion and Structure determination

The value of the molar extinction coefficient (ε) was observed to increase as the pH of the solution was increased in this experiment, while λ_{max} remained fairly constant. As can be seen from the above Figure 4.1(a) complexation in this system begins above pH 5 with the formation of MLH species which was observed to have λ_{max} 670 nm and a molar extinction coefficient (ε) of 55.6 $dm^3.mol^{-1}.cm^{-1}$. Figure 4.2 (a-c) shows various proposed possible structures for the different species, together with their theoretical (λ_{max}) calculated using Billo's method. From Table 4.3 we see that the λ_{max} observed for the MLH agrees fairly well with the λ_{max} value (i.e. 663 nm) calculated according Billo's method for two amines bound to the central metal ion (structure a) and to the reported λ_{max} (i.e. 680 nm) for the $[Cu(II)(NH_3)_2(H_2O)_4]$ species in Table 3.2 [11]. This further supports the proposed model that two amine groups are involved in coordination to Cu(II) in the MLH species. This is consistent with the conclusion from potentiometry.

The 110 species is observed to have a λ_{max} value of 600 nm with ε = 71.24 $dm^3.mol^{-1}.cm^{-1}$ and this λ_{max} value is close to that predicted for structures 4.2b and c using Billo's method. However this value is less than that of the λ_{max} $[Cu(II)(NH_3)_3(H_2O)_3]$ species which is 645 nm [11]. A similar observation was noted by Linder *et al.* for the tri-dentate complex of N, N-bis[2-(diethylamino)ethyl]-ethanediamine (i.e. moving from ML to MLH_{-1}) [12]. This conclusion is consistent with the assumption from potentiometry, which states that the ML species is formed by the coordination of three amine groups to the central metal ion. Furthermore the λ_{max} values obtained for the ML species is characteristic of equatorial coordination of amines [10]. The hydroxo species was not detected, because MLH_{-1} only starts to reach significant amounts at pH values greater than 10.

Table 3.3: Experimental lambda maximum (λ_{max}) and extinction coefficients (ε) for the PCU.Homopiperazine-Cu(II) complex.

Species	(ε) $dm^3.mol^{-1}.cm^{-1}$	(λ_{max})
1 0 0	41.6 $dm^3.mol^{-1}.cm^{-1}$	790 nm
1 1 1	55.6 $dm^3.mol^{-1}.cm^{-1}$	650 nm
1 1 0	71.2 $dm^3.mol^{-1}.cm^{-1}$	600 nm

Figure 4.2: Proposed structures for the different copper (II) complexes species with PCU.Homopiperazine with their respective wavelength max, predicted using Billo's method. The cage moety on PCU.homo is omitted for clarity:

1 1 1

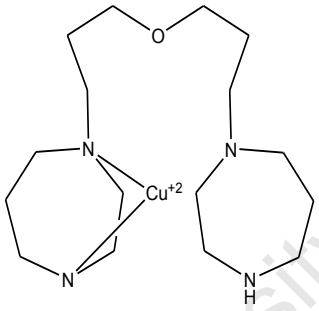

(a)

663nm

1 1 0

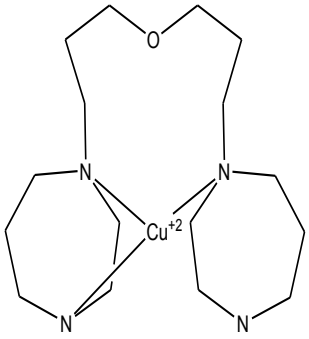

(b) 602nm

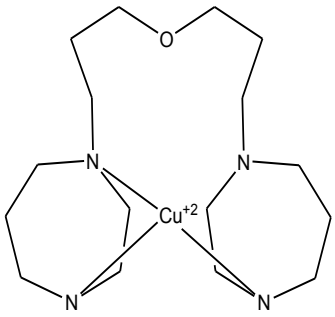

(c) 602nm

4.2 MOLECULAR MECHANICS CALCULATIONS (MM)

4.2.1 Introduction

The accurate use of UV/VIS spectrophotometry or if possible X-ray crystal structure can readily predict the structures of the copper (II) complex formed/present in solution and solid respectively with high accuracy [9]. However in order to gain more knowledge about the energies involved in the formation of the different metal ion complexes, molecular mechanics can be used. Molecular Mechanics (MM) is a tool used to calculate the strain energy introduced into a ligand by virtue of its adopted coordination geometry around a metal ion [9, 14]. These calculations of the internal strain energy of a molecule are done using force fields, but the choice of which force fields to use in a calculation is entirely dependent on the type of complex or molecule (i.e. organic or inorganic) of interest and the software program used to run the simulation [10, 12]. In a typical MM calculation each atom in the molecule is treated as an individual particle. Each particle is assigned a radius (typically the van der Waals radius), polarizability, and a constant net charge (generally derived from quantum calculations and/or experiment) [17]. Finally bonded interactions are treated as "springs" with an equilibrium distance equal to the experimental or calculated bond length and these calculations are shown in Figure 4.3 [17, 18]. The bond lengths and angles obey Hooke's law, while other interactions occurring in the complex are calculated using Lennard-Jones potentials. Some examples include dihedral angles and their equations are given in Figure 4.3. Molecular mechanics was used in this study to determine the lowest energy conformation for the metal complex species of interest and therefore account for the order of stability of the various Cu(II)-PCU.homo complexes formed in solution (i.e. M_2LH< MLH> ML) [13]. There are a limited number of reliable force fields to use for the MM calculation involving metal ions. Therefore MM calculations involving transition metal ions are not done to the same extent as organic molecules [14, 15].

Figure 4.3: force fields, which are used in this calculation, contain the energy terms listed below [Brooks et al., 1983]:

Internal energy terms:

Bonds: $E_b = \sum k_b(r - r_o)^2$ Bond Angles : $E_ø = \sum k(ø - ø_ø)^2$

Dihedrals: $E_Θ = \sum k_Θ - k_Θ \cos(nΘ)$

Non-bonded interactions:

Van der Waals: $E_{nb} = \sum [A_{ij}/r_{ij}^{12} - B_{ij}/r_{ij}^{6}]sw(r_{ij}^2, r_{on}^2, r^2_{off})$

Electrostatic: $E_{el} = \sum q_i q_j / 4\pi\varepsilon_0 r_{ij}$

Where: r, Θ, ø, and r_{ij} are bond length, bond angle, dihedral angle and inter-nuclear distance respectively. Therefore the full internal energy expression can be summarized as:

$\sum U_{total} = (E_b + E_ø + E_ø + E_{vdW} + E_{el})$

However the MM calculations of internal strain energy does not take into account two important energy quantities which contribute towards complex stability involved in the coordination of copper (II) in solution. These are entropy changes/chelate effect and electronic energy through ligand field stabilization energy. For Cu(II) Jahn-Teller distortion is rarely included in the force field.

In this study MM calculations the esff force field was used. The different chemical species in solution were constructed using the BUILD module of the Accelrys Biosym/MSI software package and were based on the speciation models obtained from UV/Vis spectroscopy and potentiometry. Geometry optimization and energy calculations were performed using the Discovery module.

Figure 4.4: Possible conformations for the different species formed by the Cu (II)-PCU.homopiperazine calculated using Insight (II). Table 4.4 lists the different contributions to the strain energy.

MLH

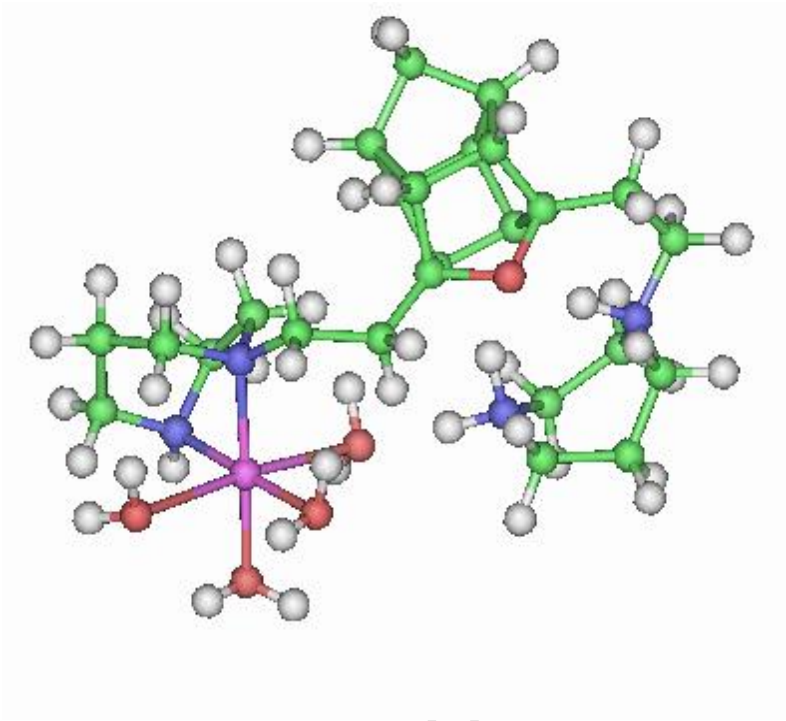

(a)

ML

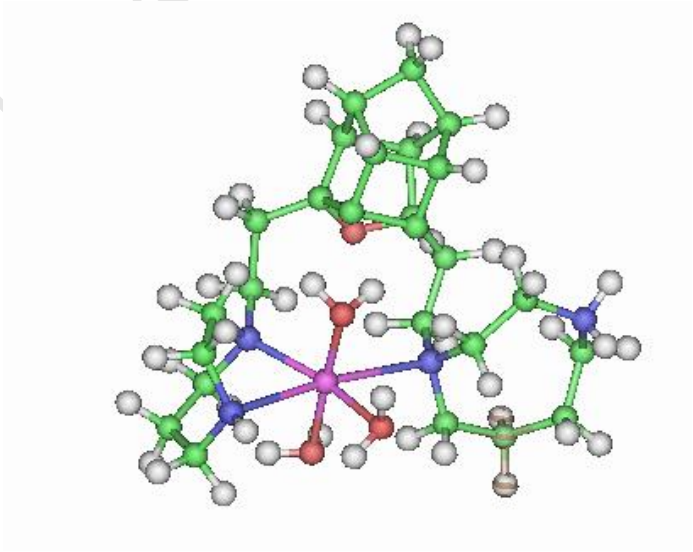

(b)

ML

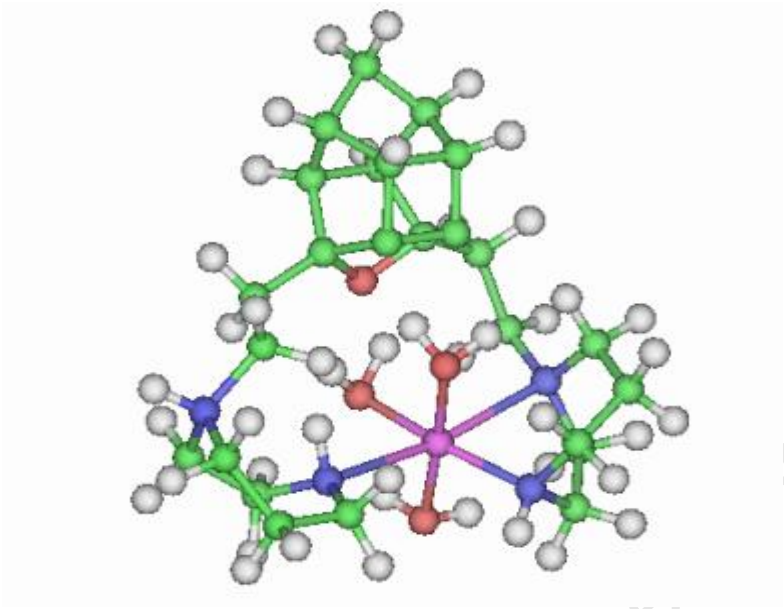

(c)

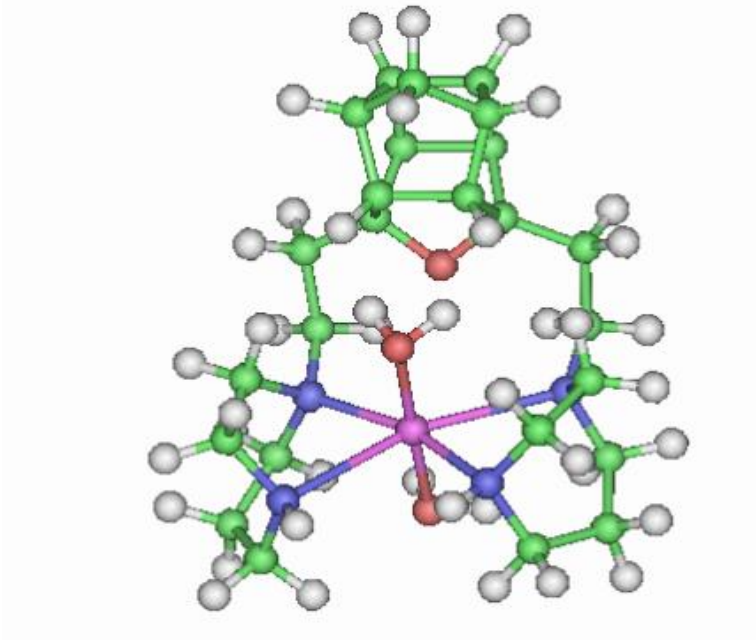

(d)

4.2.2. Results and Discussion

Figure 4.4 shows the different proposed species present in solution. The internal energies of the possible structures for the different metal complexes were calculated using the esff force field, reported in Table 3.4 [11]. Structures a, and b are the two possible coordination geometries for the MLH species, with total potential energy of 113.15 kcal $mol^{-1}$and 163.54 kcal mol^{-1} respectively. In structure 'b', three amine groups are coordinated to the metal ion. These include one terminal amine, with the other terminal amine still protonated and both tertiary amines bound to the metal ion. In 'a' only one side of the ligand is involved in coordination. Comparing the change in internal energies given in Table 4.4, for structures 'a' and 'b', structure 'a' was chosen as the most likely representative structure for the MLH species and this is consistent with the structure proposed from UV/Vis spectroscopy. The large energy contribution to the total internal energy in structure 'b' was due to the large bond deformation energy and the relative high torsion energy, which is believed to be caused by the ligand when coordinating to the metal ion because of the cyclic nature of the ligand moiety. The ML species is believed to be formed from the coordination of more amine groups around the metal ion. This species is present in significant amounts at pH's > 8, therefore we expect that all amines are either coordinated to the central metal ion or they are deprotonated. The representative structures for the ML species are shown in Figure 4.3 (c-d) with their corresponding energies given in Table 3.4. Structure 'c' has an internal energy of 143 kcal mol^{-1}, and its coordination geometry is proposed to involve three amines groups coordinated to the Cu(II) ion. However, in the alternative structure 'd', all four amines are coordinated to the metal ion forming 2 highly strained five membered contiguous chelate rings and a ten member ring (i.e. a [5, 10, 5]) system with an internal energy of 211.73 kcal mol^{-1}). Based on the MM calculations it seems that PCU.homopiperazine is not a tetradentate ligand, but behaving as a tridentate ligand. This structure is consistent with the structure of the ML species determined from UV/Vis and NMR spectroscopy.

Table 3.4. The total internal energy (E_{int}), bond, angle bending (angles), bond twisting (tortion) and out of plane (Oop) distortion energies ($kcalmol^{-1}$) for the free ligand, MLH and ML species.

Species	Bond	Angle	Torsion	Total energy	Change in internal energy free ligand to complex
Free ligand [LH_4]	4.29	42.36	30.79	77.44	
[MLH] (a)	15.20	62.25	35.68	113.15	35.70
[MLH] (b)	38.92	88.28	36.33	163.54	86.09
[ML] (c)	11.12	94.40	42.35	147.90	70.45
[ML] (d)	97.61	71.05	43.04	211.73	134.28

Reference:

1. I.D. Campbell and A.D. Dwek, Biological spectroscopy, 1984, Benjamin/Cummings, California
2. D.R Williams, The Metals of Life, , Nortrand/Reinhold, 1917,London
3. J.D Lee., Concise Inorganic Chemistry, 4th ed., Prentice Hall, 1991, London
4. V. Balzani and V. Carassiti, Photochemistry of coordination Compounds, 1970 Academic press, New York.
5. P.W.Atkins, Physical Chemistry. 1982 Oxford University Press, London.
6. S. Odisitse, MSc Thesis, 2003, University of Cape Town, South Africa.
7. A. Voye., PhD Thesis, 1993, University of Cape Town, South Africa.
8. Jackson G.E., Voye A., Kelly M., J. Inorg Biochem., 79 **(**2000) p.147-152.
9. E.J. Billo, J. Inorg . Nucl. Chem. Lett., 10 (1974) p.613.
10. A.B.P Lever, Inorganic Electronic Spectroscopy, 1968, Elservier, Switzerland
11. H. H. Jaffe and M. Orchin, Theory and Applications of Ultraviolet spectroscopy, (1962), Wiley, New York.
12. G. E. Jackson, P. W. Linder and A. Voye, A potentiometric and spectroscopic study of copper(II) diamidodiamino complexes. J. Chem. Soc. Dalton Trans., (1996), p. 4605-4612.
13. S.J.C Bailar, H.J. Emeleus, R.M. Nyholm, and A.F.T Dickenson., Comprehensive Inorganic Chemistry, (1973), Pergamon Press, Oxford .
14. E. T. Nomkoko, G. E. Jackson, B. S. Nakani and S. A. Bourne, Computer simulation of nickel in the blood-plasma following the in vitro investigation of complex formation chemistry with polyamine (amide) ligands. Dalton Trans. (2004) p.1789-1796.
15. T.E. Nomkoko, G.E. Jackson, B.S. Nakani and R. Hunter. Solution chemistry of 1,15-bis(NN-dimethyl)-5,11-dioxo-8-(N-benzyl)-1,4,8,12,15-pentaazadecane with metal ions

of biological interest-Insights toward active metal ion containing therapeutic and diagnostic agents., Dalton Trans., (2006) p.4029-4038.

16. John N. Zvimba, Graham E. Jackson, J. Inorg. Biochem, 101 (2007) p.1120-1128.
17. S. Odisitse, G. Jackson, T. Govender, H. Kruger and A. Singh, Chemical speciation of copper (II) diaminediamide derivative of pentacycloundecane-a potential anti-inflammatory agents, Dalton Trans., (2007) p.1140-1149.
18. Insight (II) 97.2, Molocular Simulation Inc. (1998) San Diego, USA, .
19. B.R Brooks, R.E Bruccoleri, D.B Olafson, D.J. States, S.Swaminathan, M. Karplus, J. Comp. Chem., (1983), p.187-217.

CHARPTER 5

IN VIVO MODELLING AND *IN VITRO* DERMAL ABSORPTION STUDIES

5.1 *In vivo* modelling

5.1.1 Introduction

The nutritional and pharmacological activity of trace metals has been reported extensively in the literature [1]. It has also been well demonstrated that Cu(II) complexes are effective in treating inflammation associated with rheumatoid arthritis and this pharmacological effect was first associated with the free labile copper (II) concentration in the body by Sorenson *et al.* in 1976. In human blood plasma and other biological media, copper (II) ion is present with its majority fraction irreversibly incorporated into metalloproteins, reversibly bound to, human serum albumin, with the remaining fraction of the metal ions bond loosely to low molecular mass ligands (e.g. carbonates, sulphates, phosphates, amino acids) or existing to a very small extend as free metal ions [2]. These l.m.w complexes are believed to exist in equilibrium with other similar free l.m.w ligands and this multicomponent system exists in constant competition for free metal ion in the blood plasma and therefore control the biological potential of the metal *in vivo* [2, 3]. L.m.w complexes are thought to have numerous biological roles, this includes being (i), involved as intermediates in some metal transport process; (ii) l.m.w complexes are also involved in the transportation of metal ion between cells in the body; (iii) or they may be required to keep certain metal in solution until the metal is needed by the body [2]. As a consequence, free metal ion or its aqua complex exists at very low concentrations. This presents researchers in this field with two problems in measuring the concentration of free metal in solution, (i) since its concentration is very low it cannot be measured using current conventional analytical methods. Also due to the very large number of ligands (i.e. proteins) and other metal complexes present in blood plasma it is difficult to separate the components using modern separation methods [2]. Furthermore, the use of probes to monitor equilibrium concentration might disrupt the equilibria that are being monitored. Based on the reasons discussed above it is not surprising how the use of computer aided simulation of metal ion-l.m.w equilibria has increased in literature. A blood

plasma model was developed by May *et al.* and has been successfully used to account for several processes in drug therapy [3]. The blood plasma data base consist of seven metal ions, forty ligands, 250 published mononuclear binary constants measured under physiological conditions, with another 400 measured under non-physiological condition and 100 ternary complex constants. Most complexes of blood plasma are charged and therefore need a neutral transport molecule that will help them cross the lipid bilayer found in cell membranes. The May model uses a program called ECCLES (Evaluation of Constituent Concentrations in Large Equilibrium Systems) to execute its calculation. ECCLES calculates the plasma mobilising index, which refers to the extend to which a particular ligand can mobilize a specific metal in the plasma without disrupting other metals ions present in blood or disrupting the equilibrium that is found to exist in the body [3].

The ligands investigated in this study have been shown to form more stable complexes with Cu(II), than with Zn(II), but this does not mean that the ligands will bind copper selectively *in vivo*. As a result modelling studies are necessary to enable us to study how PCU.homopiperazine will compete in the body system against other ligands [4]. In order to determine the efficiency of our ligands in mobilizing copper *in vivo*, the plasma mobilizing index of these ligands was investigated by using the plasma modelling program ECCLES [3, 4].

5.1.2 The plasma mobilizing index (P.M.I)

Plasma mobilizing index (p.m.i) is the ability of a specific ligand to increase the l.m.w. concentration of a specific metal *in vivo*. P.m.i is given by the following expression:

p.m.i. = (total concentration of l.m.w metal ion complexes in the presence of the drug) / (total concentration of l.m.w metal ion complexes in normal plasma)

The log p.m.i is normally plotted against the log of the concentration of the ligand. Therefore a high value of log p.m.i at low ligand concentration for any ligand-metal system indicates that the

ligand is a very good competitor against other potential ligands present in the blood plasma for the metal ion of interest [2].

Blood-plasma modelling was carried out by incorporating the formation constants determined in this study into the blood plasma model and this large database was then interrogated by ECCLES to determine the p.m.i as a function of ligand concentration [1, 3].

Zn(II) was not included in the model because it was found not to coordinate to PCU.homo The results are shown in Figure 5.1

Figure 5.1(a). P.m.i curve for PCU.homopiperazine and homopiperazine in blood plasma at pH 7.43. (b) p.m.i curve calculated for different ligands in blood plasma.

(a) (b)

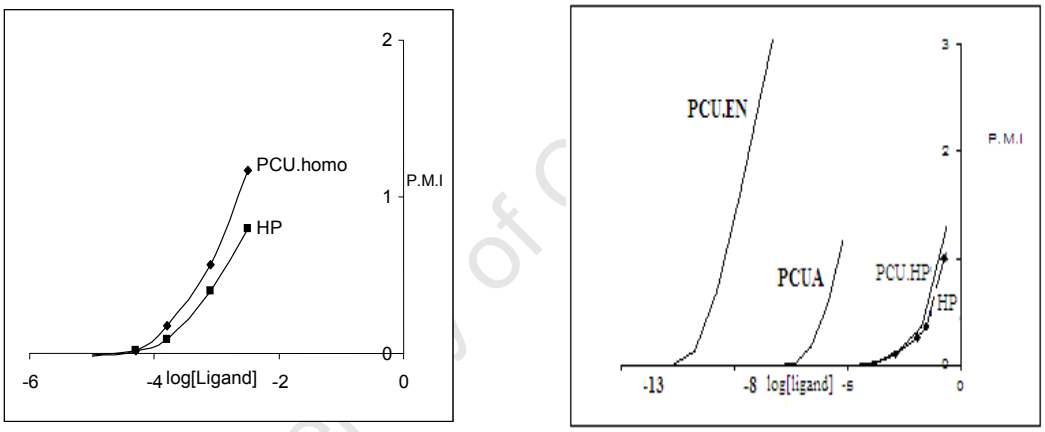

Figure 5.1(a) shows the p.m.i curves for Cu (II) plotted against the log [PCU.homopiperazine] and [homopiperazine] respectively. Figure 5.1(b) shows the log p.m.i curves as a function of log [LIGANDS] for a series of related ligands. As can be noticed from Figure 5.1(a) the p.m.i curve for PCU.homo runs slightly on top of the HP curve, thus indicating an increased p.m.i activity for the PCU.homo system. Thi is a consequence of the increase in the complex stability observed in moving from homopiperazine to PCU.homo. Another reason for the increased p.m.i value for PCU.homo over the HP system, might be the increased donor power (i.e. increased pK_a values for the amine groups) observed for PCU.homo. However PCU.homo mobilizes copper (II) to a small extend when compared with other pentacyclo-undacane (PCU) related derivatives (see

Figure 5.1(b)), with its Cu(II) p.m.i curve rising above 1 with 10^{-2} M ligand concentration used. This means that despite PCU.homo being highly selective for Cu(II) coordination in aqua solution, it is not good enough in mobilizing copper (II) *in vivo*, and the reason for this may be due to the fact that PCU.homo forms weak complexes with copper (II) when compared to the other related penta-cycloundecane derivatives, see Figure 5.1 (b).

From Figure 5.1(b) we are able to see that PCU.EN (N-4-donor) N, N'-bis [ethylene diamine]-4-[oxahexacyclododecane] and PCUA (N-4 donor) 3.5-bis [ethanediamine]-4-[oxahexacyclododecane], are 6 and 3 orders of magnitude better at mobilizing Cu(II) *in vivo* than PCU.homo (N3-donor) respectively [2]. Therefore PCU.homopiperazine cannot be used effectively to endogenously increase the l.m.w. copper (II) fraction in the body.

5.2. Dermal Absorption (*in vitro)*

5.2.1 Introduction

Low levels of bio-available copper in the blood have been associated with the development of chronic inflammation and with remission of symptoms seen with the administration of exogenous copper supplements [5, 6]. The use of copper bangle to suppress inflammation associated with RA has been known for a very long-time [5]. Walker *et al*. have measured the dermal absorption from these bracelets and found it to be significant [5]. Since then a considerable volume of literature addressing skin absorption of metal-based chemicals as the key to the observed beneficial biochemical and pharmaceutical activity has been reported [6]. Despite previous successful designs of various useful copper chelating agents capable of enhancing bio-availability of copper in the blood, the challenge still remains to develop a system which can enhance exogenous dermal absorption for topical application of copper (II)-based drugs because so far the current therapy for inflammation disorder rely on intra-articular or intravenous drug injection which causes the patient discomfort [7].

The stratum corneam is the major barrier to many potential diffusing chemical species that come in contact with the skin [8]. This is because the stratum corneam has a heterogeneneous multicomponent liphophilic membrane structure; which does not allow charged species or hydrophilic compounds to pass through it [8]. However, a well established fact is that hydrophobic species can pass through a lipid membrane. Solomon *et al.* have shown that the use of neutral complexes of copper-dihistidine increases the absorption of copper in cells of children with menkes disease with the copper complex administered intravenously [9]. Furthermore Jackson *et al*. have also shown that incorporating hydrophobic groups on the ligand significantly enhances the absorption of copper complexes across lipid-membranes and the subsequent endogenous transportation of the metal ion [10, 17]. It is important to note that hydrogen

bonding or non-covalent interaction with the skin proteins will have an effect on the passage of chemical species through the stratum corneam [10, 11, 17].

5.2.2 Diffusion

The mechanism by which chemicals passively diffuse across a lipid-membrane and the rate of passage is described by Ficks law [11, 14],

$J = dM/S.dt.$

Where J is flux in g/cm^2, S = cross section of barrier in cm^2 and dM/dt = rate of diffusion in g/s. The flux which is defined as the amount of substance that passes through a porous membrane from region of high concentration to low concentration per unit time is related to the concentration gradient dC/dX (the driving force for passive diffuse) by the a proportionality constant, the diffusion coefficient D, and is given by the following equation :

$J = -D .dC/dX$

Where D = diffusion coefficient of a drug; C = concentration of drug in g/cm^3; X = distance in centimetres of movement perpendicular to the surface of the barrier. Furthermore dC/dX is equivalent to ($C_{OUT} - C_{IN}$) where C_{OUT} and C_{IN} are the substrate concentration inside and outside the cell. Therefore, when the concentration outside the cell is larger than inside the cell the concentration gradient dC/dX will be positive and the net movement will be into the cell.

The relation between the permeability coefficient (K_p) and the steady-state flux is calculated according to following equation:

$K_P = J/C_i$

Where C_i is the initial substrate concentration outside the cell and J is the flux. Since the permeability coefficient (K_p) is in generally a physical property of the diffusing substrates, it is depends on physiochemical parameters, such as solvent temperature, solvent viscosity, nature of substrate and mass of substrate. When expressed as depth of diffusion per unit of time (here in cm/s), it provides a basis for comparison of the relative absorption rates of diverse chemicals.

Therefore it is not surprising that permeability coefficient K_p is the best descriptor of membrane penetration of many cosmetic drugs [11-13].

5.2.3 Franz cell

The primary objective of *in vitro* dermal absorption studies is to evaluate the rate of dermal penetration or to predict the percentage of dermal absorption of an administered dose of a drug of interest [12]. This type of *in vitro* dermal absorption study has been reported to provide key insights into the relationship between skin, drug and formulation, thus resulting in the development of safe new novel drugs [12]. However to date there is little or no data involving a quantitative study of the bioavailability of copper using human skin *in vivo* [12- 13]. The major research methodology used in skin permeation studies is the Franz diffusion cell. The model is based on a vertical diffusion of a drug between a donor phase and acceptor phase with a membrane (i.e. used to model the stratum corneam) mounted between the two compartments [12]. The acceptor phase is maintained at a constant temperature of 37 ºC by circulating water from a thermostated water bath. The disadvantage of this skin model currently used to mimic the stratum corneam is that it does not fully reflect the stratum corneam multicomponent structure therefore most of the times underestimate absorption of the drug [11-13]. However, Jurij *et al.* [13] have determined the skin permeability coefficient (K_p) for glycyl-L-histidyl-L-lysine cuprate diacetate in vitro and found it to be $2.43 \pm 0.51 \times 10^{-4}$ cm/h using an isolated stratum corneum (model membrane) and therefore predicted that copper as tripeptide complex will be delivered in potentially therapeutically effective amounts for inflammatory disease. Encouraged by the copper (II) speciation results, which showed the formation of a ML species in significant amount (i.e. ≈ 70%) in solution at physiological pH range (i.e. between pHs 7.3-8.5) (see Figure 6.5 (a)) dermal absorption of Cu(II)-PCU.homo has been studied. The rigid hydrophobic cage structure is believed will improve the dermal absorption of copper (II). Pehourcq *et al*. [14] have determined the partition coefficient (K_{ow} 0.618) for Cu(II)-PCUA complex at pH 7.4 a derivative

of PCU.homo and when compared to other complex in their study it was reported that the K_{ow} for PCUA was higher due to the presence of the rigid cage. *In vitro* dermal absorption studies for the Cu(II)-PCU.homo were done using a modified Franz diffusion cell (i.e. a horizontal design). A modified Franz cell was used in this study because setting up an industrial Franz cell is difficult and impractical because of its vertical design and it also requires large sample volumes.

It is important to note that the porous lipid membrane used in drug diffusion studies must have the following physicochemical properties hydrophobicity, rate limiting properties like the stratum corneam and must have negligible resistance (i.e. small lag time) to the drug diffusion through, so as to not mask the effect the drug has on the diffusion of the metal ion [5, 8].

5.2.4 Franz diffusion cells apparatus

The drug diffusion test were undertaken at room temperature on a validated tailor made Franz cell. This apparatus is made of glass and consists of two compartments, a donor phase, where a model membrane lipidic system was placed and an acceptor phase where solutes accumulate after crossing the membrane barrier. The acceptor phase was in close contact with the membrane during the experiment and was kept at physiological pH of 7.2. The effective diffusion area was 3.14 cm^2 and the volume of the acceptor phase was 50 ml.

5.2.5 Preparation of the 1:2 molar ratio Cu (II)-PCU.homopiperazine complex (diffusant).

The solution of the approximately 1:2 (v/v) molar ratio copper complex was prepared from standards in deionized water, by adding 10 ml of 10 mM copper (II) solution to 20 ml of 7.6 mM PCU.homopiperazine solution (prepared and standardised using Gran plot see Chapter 2). The pH of the solution was then raised to 7.2 by adding small amounts of NaOH solution and stored in a glass vial for use in Franz cell.

5.2.6 Preparation of a membrane for use in Franz cell.

In this study the Franz cell was used with a synthetic membrane, which was used to mimic the human skin. The lipid membrane was prepared by soaking trimmed circular discs of Watman filter paper into a Cerasome 9005 (purchased from Lipoid GmbH Germany) membrane solution for 3hrs and taken out with tweezers to dry over air. Each membrane was weighed before being used in the experiment.

5.2.7 Franz diffusion cell studies and sample analysis.

In this method, the cell consisted of two compartments of the same height and diameter, that is a donor phase cell (containing the 30 ml of copper (II)-ligand solution in water at pH 7.2) and the acceptor phase (containing deionized water at the same pH and volume as the donor phase) with a lipid membrane sandwiched between the two compartments. The pH of the acceptor phase was maintained in the physiological range, because the lower layer of the statum cornium is maintained at physiological pH of 7-7.6. The acceptor phase liquid was kept homogenous throughout the diffusion experiment by using a magnetic stirrer. The membrane sizes (i.e. mass and thickness) were be kept constant for every new diffusion experiment undertaken. Both the air openings of the cell's compartments were closed with parafilm to prevent sample evaporation and the development of air bubbles was stopped by tilting the apparatus a little. Equal amounts (i.e. 7 ml) of samples from the donor and acceptor phase were taken using a glass syringe and poured into 10 ml glass vials at pre-set time intervals. The volumes of the liquid in both cell compartments must be maintained equal to cancel out the effects of hydrostatic pressure on the diffusion of the copper (II) complex in solution throughout the experiment [14]. The extracted sample from the acceptor phase was then analysed using atomic absorption spectroscopy at 324,7nm for copper (II) absorbance. The cumulative amounts of the copper (II)-ligand in the acceptor phase were then plotted against time, to obtain the flux of the copper (II)-complex.

5.3 Results and discussion

5.3.1Franz cell

The accumulative amounts of Cu(II)-homopiperazine and Cu(II)-PCU.homopiperazine per unit area across cerasome 9005 membrane over 24 hrs are plotted in Figure 5.2. The flux values, permeability coefficient and their corresponding standard deviation (SD) of two complexes are shown in Table 5.1. From Figure 5.2, it can be seen that the diffusion of the copper complexes is very slow for the first 8 hours of the experiment. This is followed by a further phase of rapid diffusion called the steady state from 8 to 24 hours. The reason for the observed induction period was attributed to the development of equilibrium between the donor phase and the membrane as a result of the complex diffusing through it [11, 17].

Figure 5.2(a). Plots of Copper diffusion of Cu(II)-homopiperazine and Cu(II)-PCU.Homopiperazine through cerasome 9005 membrane. (b) Plots of copper diffusion of CuPCU.homo, CuGly (copper(II)- Glycinate), CuH(555-N) (copper(II)- N-(2-(2-aminoethyl)ethyl)picolinamide), and CuDTPA (copper(II)- diethylenetriamine-N,N,N',N'',N"-pentaacetic acid.

(a) (b)

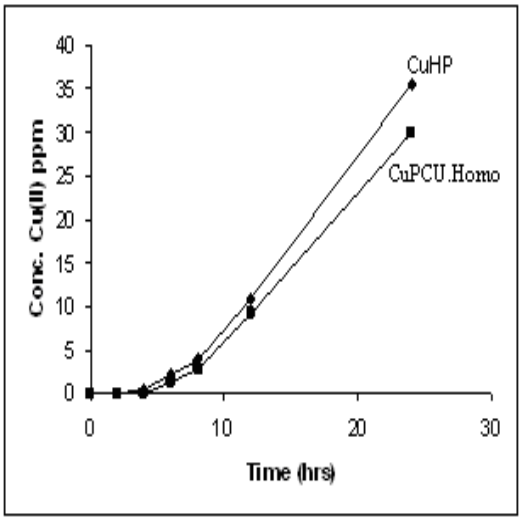

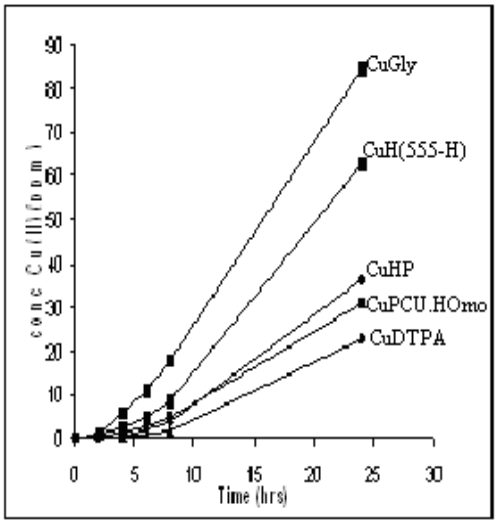

Upon comparing the diffusion process of CuPCU.homo, CuGly (copper(II)- Glycinate), CuH(555-N) (copper(II)- N-(2-(2-aminoethyl)ethyl)picolinamide), and CuDTPA (copper(II)-diethylenetriamine-N,N,N',N'',N"-pentaacetic acid, each complex showed a similar trend (i.e. biphasic diffusion behaviour) as shown in Figure 5.2(b) which was also concluded as being caused by the development of a equilibrium between the donor phase and the membrane.

5.4.2 Flux (J) and permeability coefficient (K_p) calculations

The steady states flux and permeability coefficients of Cu(II)-PCU.homo were calculated from the gradient of the curves in Figure 5.2 (a). The flux obtained for the Cu(II)-PCU.homopiperazine complex and the values of other copper (II) complexes from literature are reported in Table 5.1, where flux is expressed by J (mean ±SD) 10^{-9}g/cm^{2}s, concentration (ppm) and permeability coefficient K_p (mean ± SD) 10^{-6} cm/s.

Table 4.1. Summary of average Cu(II) complexes flux J (mean ±SD) 10^{-9}g/cm^{2}s and permeability coefficient K_p (mean ± SD) 10^{-6} cm/s through cerasome 9005 membrane

Complexes	J (mean ±SD) 10^{-9}g/cm^{2}s	K_p (mean ± SD) 10^{-6} cm/s	Ref
CuPCU.homo	1.07± 0.04	5.06± 0.03	
CuHP	1.79± 0.01	5.63± 0.04	
CuDTPA	0.690± 0.004	2.17± 0.01	14
CuPrDH	0.724 ± 0.003	2.28± 0.01	14
CuGly	1.84±0.01	5.79±0.04	14
CuH(555-N)	2.412±0.01	7.60±0.03	14

Figure 5.3. The influence of various ligand systems on the flux of copper ions through a cerasome 9005 membrane lipid membrane.

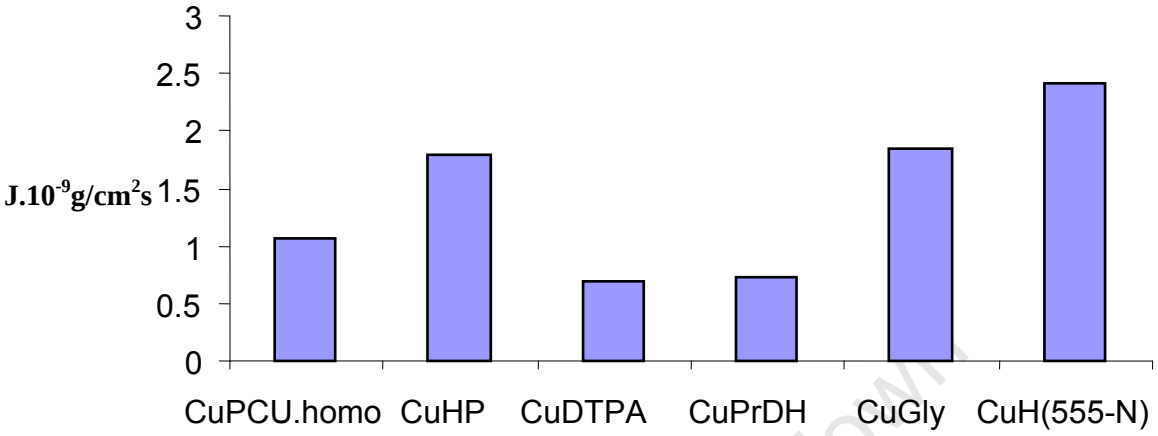

Figure 5.3 shows the influence of the different ligand systems on the flux of copper ions through the cerasome membrane. These results suggest that the complexation of Cu(II) ions by the different ligands greatly influences the diffusion of copper ions across the membrane, because different flux values are obtained for different copper (II) complexes studied. The following order of CuH(555-N) > CuGly > CuHP > CuPCU.homo > CuPrDH > CuDTPA was obtained. Comparing the permeation coefficient K_P of copper complexes of PCU.homopiperazine and homopiperazine, there is a decrease in K_p in moving from homopiperazine to PCU.homopiperazine and this was attributed to the higher molecular weight of PCU.homopiperazine. A similar effect of molecular weight (MW) of complex on the flux of copper complexes was also observed and reported by Potts *et al*, and this effect can be obtained quantitatively from their equation based on two physicochemical properties of octanol-water partition coefficient $\log K_{ow}$ and molecular weight MW of complex and is given by the linear relationship [11],

$$\text{Log } K_p = \log (D^o/h) + f \log K_{ow} - \beta MW$$

Where D^o represents the diffusivity of a hypothetical molecule having zero molecular weight, h is the membrane length in cm and β is a constant.

Table 4.2: Physicochemical parameters and Permeability coefficient (K_p (mean ± SD) 10^{-6} cm/s) of 6 copper (II) complexes

Complexes	Molecular Weight (MW) g/mol	K_p (mean ± SD) 10^{-6} cm/s	% Cu complex concentration (ppm)	Log β	-Log K_{ow} [14]
CuPCU.homo	416.51 g/mol	5.06± 0.03	80 MLH	9.25	
CuHP	163.14 g/mol	5.63± 0.04	100 ML	7.60	3.49±0.01
CuDTPA	414.77 g/mol	2.17± 0.01	70 ML	8.69	3.62±0.01
CuPrDH	314.79 g/mol	2.28± 0.01	100 MLH_{-1}	5.00	3.45±0.02
CuGly	138.566 g/mol	5.79±0.04	100 ML_2	8.15	2.661±0.003
CuH(555-N)	288.768 g/mol	7.60±0.03	100 MLH_{-1}	11.513	3.005±0.007

Table 5.2 is the summary of Molecular Weight (MW), % Cu complex concentration (ppm), Log β, and the permeation coefficient K_p (mean ± SD) 10^{-6} cm/s of the four copper (II) complexes. It has already been established by Jackson *et al.* that the diffusion (K_p) of the five copper (II) complexes (i.e. CuH(555-N), CuGly CuHP, CuPrDT and CuDTPA) across cerasome 9005 membrane is linearly dependent on their octanol/water partion coefficient K_{ow}, with K_p increasing with the increase in K_{ow} [13]. Therefore in this study it was assumed that permeation coefficient (K_p) of CuPCU.homo too is affected by its K_{ow}, since Pehourcq *et al.* [11] showed how the addition of a hydrophobic rigid cage on a Cu(II)-polyamine-diamine complex drastically improves the partion coefficient K_{ow} of this polyamine-diamine complexes. A value of Log K_p = -5.30 ± 0.03 obtained for CuPCU.homo in this study and was comparable to the value Log K_p = -7.17 ± 0.51 reported by Hostynek *et al*. for the diffusion of a copper (II)-tripeptide complex in vitro using isolated stratum corneam [8], therefore giving confidence to the result obtained. From Table 4.2, since the permeability across the lipid membrane of the each complex is affected by its hydophobicity, it is not surprising that the permeation coefficient K_p of CuGly is higher

than for Cu-PCU.homo because the latter complex in solution at pH 7.2 it exists as a charged species (MLH) while CuGly exists as a neutral ML_2 (100%) species at the same pH value. Similarly Kobayashi *et al.* [15] have also reported that the human nail permeability of several model drug derivatives of p-hydroxybenzoic acid esters where markedly decreased in the ionic homologues than in their non-ionic homologues. For example the K_p of pyridine (K_p 6.36 x 10^7 cm/s of non-ionic) and K_p for Mexilentin hydrochloride (K_p 0.202 x 10^7 cm/s of ionic) [14].

.

Reference:

1. D. R.William,'The Metals of Life,' Van Norstrand Reinhold, London, 1971
2. S. Odisitse, G. E. Jackson, T. Govender, H. Kruger and A. Singh. Chemical speciation of copper (II) diaminediamide derivative of pentacycloundecane-a potential anti-inflammation agent. Dalton Trans., (2007), p.1140-1149.
3. D. D Perrin and R. P. Agarwal in 'Metal Ions in Biological Systems,'ed. H. Sigel, Marcel Dekker, New York, 2 (1973) p. 168
4. M. P. May and P. W. Linder. Computer Simulation of Metal-ion Equilibria in Biofluids: Models for the low-molecular-weight Complex Distribution of Calcium (II), Magnesium (II), Manganese (II), Iron (II), Copper (II), Zinc (II), and Lead (II) ions in Human Blood Plasma, Dalton Trans, (1977), p.588-595
5. J. E. Weder , C. T. Dillon , T. W. Hambley , B. J. Kennedy, P. A. Lay , J. R. Biffin , H. L. Regtop , N. M. Davies -Copper complexes of non-steroidal drugs.- a Centre for Heavy Metals Research, (2006) School of Chemistry University of Sydney, Sydney NSW, Australia
6. J. R. J.Sorenson in metal ion in biological systems, 4 (1982) H. Sigel(Ed), Marcel Decker, New York
7. N, J. Zvimba, and G. E. Jackson, Copper chelating anti-inflammatory agents N^1-(2-aminoe ethyl)-N^2-(pyridin-2-ylmethyl)ethane-1, 2-diamine ([555-N]) and *N*-(2-(2-aminoethylamino) ethyl) picolinamide ([H (555)-N]) a vitro and in vivo study. Journal of Inorganic Biochemistry. 101 (2007) p.148-15
8. J. J Hostỳnek, F. Dreher and H.I. Maibach. Human stratum corneam penetration by copper: In vivo study after occlusive and semi-occlusive application of the metal as powder. Food and Chemical Toxicology 44 (2006) p.1539-1543

9. E. I. Solomon, U.M. Sundaram, and T.E. Machonkin. Chem Rev 96 (1996).p. 2563-2605
10. E.T Nomkoko., G.E Jackson., B.S Nakani., S.A Bourne., J. Chem. Soc., Dalton Transactions, (2004), p.1789
11. Shiow-Fern Ng, J Rouse, D. Sanderson and G eccleston. A Comparative Study of Transmembrane Diffusion and Permeation of Ibuprofen across Synthetic Membranes Using Franz Diffusion Cells. Pharmaceutical, 2 (2010) p. 209-223
12. T. J Franz. Percutaneous absorption. On the relevant of in vitro data. J. Invest. Dermatol ., 64, (1975) p.190-195
13. J. J Hostỳnek, F. Dreher and H.I. Maibach. Human skin penetration of copper tripeptide in vitro as a function of skin layer. G.P. Moss, J.C. Dearden, H. Patel and M.T.D. Cronin. Quantitative structure-permeability relationships (QSPRs) for the percutaneous absorption. Toxicology in Vitro, 16 (2002) p.299-317
14. L. Mazurowska, K. Nowak-Buciak and M. Mojski. ESI-MS method for the in vitro investigation of skin penetration by copper-amino acid complexes: from an emulsion through a model membrane. Anal Bioanal Chem. 388 (2007) p. 1157-1163
15. F. Pehourcq, M. Matoga, C. Jarry and B. Bannwarth, J. Liq. Chromatogr. Relat. Technol. 24 (2001) p. 2177
16. M. Herd, J Camakaris, R. Cristofferson, P Wookey and D.M. Danks. Uptake and efflux of copper-64 in Menkes-disease and normal continuous lymphoid cells lines. J. Biochem. 247 (1987) p.341-347
17. S. Odisitse, G. E. Jackson, T. Govender, H. Kruger and A. Singh. Chemical speciation of copper (II) diaminediamide derivative of pentacycloundecane-a potential anti-inflammation agent. Dalton Trans., (2007) p.1140-1149
18. E. Umba and G. E. Jackson. (Msc thesis 2010) University of Cape Town, South Africa: The evaluation of tissue permeability of novel copper based anti-arthritis

19. Y. Kobayashi, T. Komatsu, M. Sumi, S. Numajiri, M. Miyamoto, D. Kobaashi, K. Sugibayashi, and Y. Morimoto. *In vitro* permeation of several drugs through the human nail plate: relationship between physicochemical properties and nail permeability of drugs. Euro. J. of Pharma. Sci. 21 (2004) p. 471-477.

CHARPTER 6:

GENERAL DISCUSSION AND CONCLUSION

6. GENERAL DISCUSSION AND CONCLUSION

The equilibrium constants of H^+, Cu(II) and Zn(II) at 25˚C in 0.15 mol.dm-3 [NaCl] with ligands, homopiperazine and PCU.homopiperazine were investigated using glass electrode potentiometry.

Potentiometric data analysis using ESTA showed that PCU.homopiperazine takes four protons in the pH range 2-11. Furthermore PCU.homopiperazine presents two of its secondary amines as moderate to strong bases with the remaining amines behaving as weak bases. This trend is consistent with many reported protonation sequence of polyamine systems. The observed protonation constants agreed with those from related tetra-amine ligands and their analogues. The reasonably low standard deviation in the log β_{pqr}'s and the low Hamilton R-factor give confidence to the chosen model to explain the protonation system of PCU.homopiperazine. Furthermore, from NMR spectroscopy studies, the graphs of chemical shifts as function of solution pH were successfully used to obtain the micro-protonation constant of the terminal amines pK_a = 10.1 and 9.0. These are comparable to the first two protonation constants on PCU.homopiperazine determined from potentiometry.

PCU.homopiperazine formed more stable complexes with copper (II) than with zinc (II). The tetragonally distorted ML species was the dominant species under physiological conditions. The tetragonally distorted arrangement of PCU.homopiperazine with three donor atoms around the copper (II) ion with λ_{max} and ε equal to 600nm and 71.24 $dm^3mol^{-1}cm^{-1}$ respectively, has been suggested on the basis of UV/Vis spectrophotometric measurement (see Figure 4.1(b)) and Billo's test. This preferred coordination geometry in ML species was further supported by NMR spectroscopy and MM calculations. The weak stability in the Zn(II)-PCU.homopiperazine system was attributed to being caused by the cyclic nature of the ligand 'homopiperazine' which is believed to find it difficult to form a tetrahedral geometry around zinc(II) ion, and this leads to a weaker complex being formed.

The primary objective of this study was to produce a drug which is able to mobilize Cu(II) in blood plasma. Zn(II) and Ca(II) ions, being present in the blood plasma in large concentrations are regarded as potential competitors of Cu(II) *in vivo*. Since no complexation was detected for the Zn(II)-PCU.homopiperazine system, it was not included since these metal ions would not compete effectively in vivo. The plasma mobilising index of PCU.homopiperazine was determined and compared to p.m.i of Homopiperazine. The order of metal ion selectivity and mobilizing ability of these two ligands is given by PCU.homopiperazine > homopiperazine. However the model showed that PCU.homopiperazine is not good in mobilizing copper *in vivo*, with 0.01M needed to cause a 10 fold increase in the l.m.w concentration of Cu(II). It was also established that PCU.homopiperazine is between 4 and 6 orders of magnitude poorer in mobilizing copper (II) when compared to the previously studied related pentacyclo-undacane (PCUA) derivatives. Therefore PCU.homopiperazine-Cu(II) complexes is predicted to dissociate in blood plasma. However all was not lost as the ligand could still be used to improve the dermal absorption of copper (II).

A simple empirical model of the skin was constructed for predicting the *in vivo* permeability coefficient in water at pH 7.2, for the transdermal delivery of CuGly, CuH(555-N), CuPCU.homo, CuHP, CuPrDT and CuDTPA respectively. CuH(555-N) was found to increase the dermal absorption of copper (II) the most when compared to the rest of the ligand systems in this study with $K_p = 7.60 \times 10^{-6}$ cm/s. The permeability across the lipid membrane of the CuPCU.HP complex was concluded to be affected by its hydrophobicity. The permeation coefficient K_p of CuGly ($K_p = 5.79 \times 10^{-6}$ cm/s) is higher than that of Cu-PCU.homo ($K_p = 5.06 \times 10^{-6}$ cm/s) because the latter complex in solution at pH 7.2 exists as a charged species MLH while Cu-Gly exists as an ML_2 (100%) species at the same pH value. A value of Log $K_p = -5.30 \pm 0.03$ obtained for CuPCU.homo in this study and was comparable to the value Log $K_p = -7.17 \pm 0.51$

reported by Hostynek *et al*. for the diffusion of a copper (II)-tripeptide complex in vitro using isolated stratum corneam, therefore giving confidence to the results obtained in this study.

Judging from the result obtained in this study, more work has to be done in developing new knowledge and understanding of factors that affect the coordination of copper (II) chelating agents, so as to improve the efficacy of the copper complexes used in the alleviating inflammation associated with R.A.

APPENDIX

LIST OF FIGURES:

Figure 5.3: The influence of various ligand systems on the flux of copper ions through a cerasome 9005 membrane lipid membrane.

LIST OF TABLES